# Duplicated KAI2 receptors with divergent ligand-binding specificities control distinct developmental traits in *Lotus japonicus*

**Samy Carbonnel[1,2], Salar Torabi[1,2], Maximilian Griesmann[1], Elias Bleek[1], Yuhong Tang[3], Stefan Buchka[1], Veronica Basso[1,#], Mitsuru Shindo[4], Trevor L. Wang[5], Michael Udvardi[3], Mark Waters[6,7], Caroline Gutjahr[1,2,*]**

[1]LMU Munich, Faculty of Biology, Genetics, Biocenter Martinsried, Großhaderner Str. 2-4, 82152 Martinsried, Germany

[2]Technical University of Munich (TUM), School of Life Sciences Weihenstephan, Plant Genetics, Emil Ramann Str. 4, 85354 Freising, Germany

[3]Noble Research Institute, Ardmore, Oklahoma 73401 USA

[4]Institute for Materials Chemistry and Engineering, Kyushu University, Kasugakoen-6, Kasuga, Fukuoka, 816-8580, Japan

[5]John Innes Centre, Norwich Research Park, Norwich NR4 7UH, UK

[6]School of Molecular Sciences, The University of Western Australia, 35 Stirling Hwy, Perth, WA 6009, Australia

[7]Australian Research Council Centre of Excellence in Plant Energy Biology, The University of Western Australia, 35 Stirling Hwy, Perth, WA 6009, Australia

[#]Present address: Université de Lorraine, INRA, UMR Interactions Arbres/Microorganismes (IAM), Laboratoire d'excellence Recherches Avancés sur la Biologie de l'Arbre et les Ecosystèmes Forestiers (LabEx ARBRE), Centre INRA Grand-Est, 54280 Champenoux, France.

Address for correspondence: caroline.gutjahr@tum.de

**Short title:** Ligand specificity of *Lotus japonicus* KAI2 receptors

## Abstract

Karrikins (KARs), smoke-derived butenolides, are perceived by the α/β-fold hydrolase KARRIKIN INSENSITIVE2 (KAI2) and thought to mimic endogenous, unidentified plant hormones called KAI2-ligands (KLs). In legumes, *KAI2* has duplicated. We addressed sub-functionalization of KAI2a and KAI2b in *Lotus japonicus* and demonstrate, their binding preferences to synthetic ligands differ *in vitro* and in a heterologous Arabidopsis background. These differences can be explained by three divergent amino acids near the binding pocket, two of which are conserved across legumes, suggesting legumes produce at least two KLs with different stereochemistry. Unexpectedly, *L. japonicus* responds organ-specifically to synthetic KAI2-ligands: hypocotyls respond to $KAR_1$, $KAR_2$ and *rac*-GR24; root systems respond only to $KAR_1$. In hypocotyls, LjKAI2a is required for karrikin responses, while LjKAI2a and LjKAI2b operate redundantly in roots. Our results open novel research avenues into the diversity of butenolide ligand-receptor relationships and the mechanisms controlling diverse developmental responses to endogenous and synthetic KAI2 ligands.

## Introduction

Karrikins (KARs) are small butenolide compounds derived from smoke of burning vegetation that were identified as stimulants of fire-following plant species [1]. They can also accelerate seed germination of species, that do not grow in fire-prone environments such as *Arabidopsis thaliana*. This has enabled the identification of genes encoding karrikin receptor components via forward and reverse genetics. The α/β-fold hydrolase KARRIKIN INSENSITIVE2 (KAI2), is thought to bind KARs, and the F-box protein MORE AXILLIARY BRANCHING 2 (MAX2) is required for ubiquitylation of repressor proteins via the Skp1-Cullin-F-box (SCF) complex [2, 3, 4, 5, 6]. In addition to delayed seed germination, Arabidopsis *kai2* mutants display several developmental phenotypes, including increased hypocotyl length, reduced cotyledon and rosette leaf area, a thinner cuticle, reduced root hair length and density and increased root skewing and lateral root density [4, 7, 8, 9, 10]. Moreover, mutants deficient in either the homologue of *KAI2* (*D14-LIKE*) or the homologue of *MAX2* (*D3*) mutants are perturbed in colonization by arbuscular mycorrhiza (AM) fungi [11]. These phenotypes, unrelated to smoke and germination, suggest the existence of endogenous signalling molecules, provisionally called KAI2-ligands (KLs) that bind to KAI2 and regulate development and AM symbiosis, and are mimicked by KARs [7, 12]. There are six known KARs, of which $KAR_1$ is most abundant in smoke-water [1, 13]. $KAR_1$ and $KAR_2$ are commercially available and commonly used in research. $KAR_1$ differs from $KAR_2$ by an additional methyl group at the butenolide ring [14].

Perception of KARs is very similar to that of strigolactones (SLs), apocarotenoids, which were originally discovered in root exudates in the rhizosphere [15], where they act as germination cues for parasitic weeds [15] and as stimulants of AM fungi [16]. In addition to their function in the rhizosphere, SLs function endogenously as phytohormones and

repress shoot branching [17, 18]. They have also been suggested to affect lateral and adventitious root formation, root-hair elongation, secondary growth and nodulation reviewed in [19, 20].

SLs are perceived by the α/β-fold hydrolase D14/DAD2 that, like KAI2, interacts with the SCF-complex via the same F-box protein MAX2 [21, 22] to ubiquitylate repressors and mark them for degradation by the 26S proteasome. The currently most likely repressors of karrikin/KL and SL signalling belong to the SUPPRESSOR OF MAX2 1-LIKE (SMXL) protein family and are closely related to class-I Clp ATPases [23, 24, 25]. They contain a well-conserved ethylene-responsive element binding factor-associated amphiphilic repression (EAR) motif, which interacts with TOPLESS proteins that act as transcriptional co-repressors [25, 26, 27]. Thus, it appears that SL and KAR/KL signalling may function in releasing transcriptional repression. In Arabidopsis the SMXL family comprises 8 members and, it is generally assumed that SMAX1 and SMXL2 (SMAX1-LIKE2) repress KAR/KL responses , while SMXL6, SMXL7 and SMXL8 (collectively represented by a single homologue in rice, D53) redundantly repress strigolactone responses [10, 23, 24, 25, 26, 27].

Phylogenetic analysis of the α/β-fold hydrolase receptors in extant land plants revealed that an ancestral *KAI2* is already present in charophyte algae, while the so-called eu-*KAI2* is ubiquitous among the land plants. The strigolactone receptor gene, *D14* evolved only in the seed plants likely through duplication of *KAI2* and sub-functionalization [28]. An additional duplication in the seed plants gave rise to *D14L2* (*DLK2*), an α/β-fold hydrolase of unknown function, which is transcriptionally induced in response to KAR treatment in a *KAI2* and *MAX2*-dependent manner, and currently represents the best-characterized KAR marker gene in Arabidopsis [4, 29]. Despite their similarity, KAI2 and D14 cannot replace

each other in Arabidopsis, as shown by promoter swap experiments [30]. This indicates that thei specific expression pattern does not determine their signaling specificity. Instead, specificity must be caused by the tissue-specific presence of their specific ligands, their ability to interact with other proteins or both.

In Arabidopsis and rice, in which KAR/KL signalling has so far been mostly studied, *KAI2* is a single copy gene. However, there are other plant species with several *KAI2* copies. For example, the *Physcomitrella patens* genome contains 11 genes encoding KAI2-like proteins. They have diversified in a loop that determines the rigidity of the ligand-binding pocket, such that some of them preferentially bind $KAR_1$ and others the SL 5-desoxystrigol *in vitro* [31]. The genomes of parasitic plants of the Orobanchaceae and the genus *Striga* also contain several *KAI2* copies. Some of these have evolved to perceive strigolactones, some can restore KAR-responses in Arabidopis *kai2* mutants, and others do not mediate responses to any of these molecules in Arabidopsis [7, 32, 33]. Together, this indicates that in plant species with an expanded KAI2-family there is scope for a diverse range of ligand-binding specificities (as well as for diverse protein interaction partners). Interestingly, even among plants with only one *KAI2* receptor gene, the responsiveness to karrikin molecules can differ significantly. For example, Arabidopsis plants respond to $KAR_2$ with increased expression of the marker gene *DLK2*, reduced hypocotyl growth and increased root hair length and density and respond more strongly to $KAR_2$ relative to plants treated with $KAR_1$ [4, 10]. In contrast, rice roots did not display any transcriptional response to $KAR_2$, not even for the marker gene *DLK2* [11]. It is unclear what determines these differences in $KAR_2$ responsiveness among distinct plant species.

Legumes comprise a number of agronomically important crops and they are unique among plants as they can form nitrogen-fixing root nodule symbiosis with rhizobia in

addition to arbuscular mycorrhiza. Given the possible diversity in KAI2-ligand specificities among plant species, we characterized the karrikin receptor machinery in a legume, the commonly used model *L. japonicus,* for which extensive reverse genetics ressources are available [34, 35]. We found that *KAI2* has duplicated in the legumes and that *L. japonicus* KAI2a and KAI2b differ in their binding preferences to synthetic ligands *in vitro* and in the heterologous Arabidopsis *kai2-2* mutant background. We demonstrate that these ligand binding preferences can be explained by three amino acids at the binding pocket, suggesting that the duplicated KAI2 receptors may have sub-functionalized to perceive different versions of endogenous KL-molecules. We found a surprising organ-specific responsiveness to synthetic KAI2-ligands, with hypocotyl development responding to $KAR_1$, $KAR_2$ and *rac*-GR24, and root system development responding only to $KAR_1$. These responses depended only on LjKAI2a in hypocotyls, while LjKAI2a and LjKAI2b operated redundantly in roots. Together these findings suggest that a diversity of mechanisms may influence KAR/KL responses including receptor-ligand binding specificity or organ-specific interaction of KAI2 with other proteins.

## Results

### *KAI2* underwent duplication prior to diversification of the legumes

To characterize the karrikin and the strigolactone perception machinery in *L. japonicus* we retrieved KAI2, D14 and MAX2 by protein BLAST using Arabidopsis KAI2, D14 and MAX2 as templates. A phylogenetic tree revealed that *LjD14* (*Lj5g3v0310140.4*) is a single copy gene whereas *LjKAI2* is duplicated in the genome of *L. japonicus*, in contrast to Arabidopsis and rice (Fig. 1), resulting in two paralogs *LjKAI2a* (*Lj2g3v1931930.1*) and *LjKAI2b* (*Lj0g3v0117039.1*). The *LjKAI2* duplication event must have occurred prior to the

diversification of the legumes or at least before the separation of the Millettioids and Robinioids [36] a similar pattern of duplication is also detected in soybean, pea and *Medicago truncatula*.

The F-box protein-encoding gene *LjMAX2* also underwent duplication likely as a result of whole genome duplication, because the two *LjMAX2* copies are in two syntenic regions of the genome (Supplementary Fig. S1a). However, only one *LjMAX2* copy (*Lj3g3v2851180.1*) is functional and the other copy *ΨMAX2-like* (*Lj0g3v0059909.1*) appears to be a pseudogene as it contains an early stop codon, resulting in a putative truncated protein of 216 instead of 710 amino acids (Supplementary Fig. S1b). It appears that an insertion of one nucleotide into *ΨMAX2-like* created a frameshift, because manual deletion of Thymine 453 restores the correct nucleotide sequence, which would allow the synthesis of a full length MAX2-like protein (Supplementary Fig. S1b).

We wondered why *L. japonicus* retained two intact copies of KAI2 and hypothesized that they may have functionally diverged, perhaps through changes in their expression pattern and/or amino acid sequence, which may cause differences in the relative spatial distribution of LjKAI2a and LjKAI2b, their ligand binding or their ability to interact with other proteins. We analysed the transcript accumulation of *LjKAI2a* and *LjKAI2b*, as well as *LjD14* and *LjMAX2* in different organs of *L. japonicus* (Supplementary Fig. S2a and S2b). Overall, both *LjKAI2a* and *LjKAI2b* transcripts accumulated to higher levels than those of *LjD14* and *LjMAX2*. *LjKAI2a* transcripts accumulated approximately 100-fold more in aerial organs than *LjKAI2b*, whereas *LjKAI2b* accumulated 10-fold more than *LjKAI2a* in roots of adult plants, which were grown in a sand-vermiculite mix in pots. However, in 1-week-old seedlings grown on water-agar in Petri dishes in short-day conditions, *LjKAI2a*

transcripts accumulated to more than 10-fold higher levels than *LjKAI2b* in both roots and hypocotyls (Supplementary Fig. S2b). This difference between *LjKAI2a* and *LjKAI2b* transcript was less pronounced in roots grown in long-day conditions. Together, this indicates that *LjKAI2a* and *LjKAI2b* are regulated in an organ-specific, age- and/or environment-dependent manner, which implies that their individual expression pattern is caused by at least partially different transcriptional regulators.

We also examined the sub-cellular localization of the four corresponding proteins in transiently transformed *Nicotiana benthamiana* leaves, using fusions with TSaphire or mOrange. Similar to observations in Arabidopsis [37, 38], TSaphire-MAX2 localized specifically to the nucleus, while the α/β-hydrolases (D14, KAI2a and KAI2b) fused to mOrange localized to the nucleus and cytoplasm (Supplementary Fig. S3a). Western blot analysis confirmed that the mOrange signal observed in the cytoplasm was due to the full-length fusion protein and not caused by free mOrange fluorophore, corroborating the dual localization of the two α/β-hydrolases (Supplementary Fig. S3b).

### *L. japonicus KAI2a*, *KAI2b* and *D14* can replace their orthologs in Arabidopsis

We examined whether LjKAI2a and LjKAI2b may have evolved ligand binding specificities and/or different functions in plant development. To examine, whether they both function in a canonical manner, we employed a well-established hypocotyl elongation assay in Arabidopsis [7, 30], after transgenically complementing the *Arabidopsis thaliana kai2-2* mutant [4] with *LjKAI2a* and *LjKAI2b* driven by the *AtKAI2* promoter. Both restored inhibition of hypocotyl elongation in the *kai2-2* mutant, however *LjKAI2b* was not as efficient as *LjKAI2a* in four independent transgenic lines (Fig. 2a). We also examined the ability of *LjD14* to restore hypocotyl growth inhibition, but as expected *LjD14* driven by the *AtKAI2*

promoter did not restore the hypocotyl length in *Atkai2-2*. However, *LjD14* restored repression of shoot branching of the Arabidopsis *d14-1* mutant [4], when driven by the Arabidopsis *D14* promoter, which was not the case for *LjKAI2a* and *LjKAI2b* (Fig. 2b and 2c). These results together with the phylogenetic tree (Fig. 1) demonstrate that *L. japonicus KAI2a*, *KAI2b* are both functional orthologues of the Arabidopsis karrikin/KL receptor gene *KAI2*, whereas *L. japonicus D14* is the functional orthologue of the *Arabidopsis* strigolactone receptor gene *D14.* Similar to the situation in Arabidopsis [30], the *L. japonicus KAI2* genes and *D14* are not interchangeable. The different ability of *LjKAI2a* and the paralog *LjKAI2b* to rescue the *Atkai2-2* hypocotyl phenotype might be due to variation in affinity to endogenous karrikin-like ligand(s) or to interacting Arabidopsis proteins caused by variations in amino acids exposed at the protein surface.

### ***Lotus japonicus*** **KAI2a and KAI2b differ in their ligand binding specificity**

To explore whether *L. japonicus* KAI2a and KAI2b can mediate hypocotyl responses to karrikins we quantified hypocotyl length of the *Atkai2-2* lines transgenically complemented with *LjKAI2a* or *LjKAI2b* after treatment with $KAR_1$ and $KAR_2$ (Fig. 3a and 3b). Two independent lines complemented with *LjKAI2a* displayed the same reduction in hypocotyl growth in response to $KAR_1$ and to $KAR_2$, similar to the line complemented with *AtKAI2*. However, the two lines expressing *LjKAI2b* responded more strongly to $KAR_1$ than to $KAR_2$, contrasting with the common observation, that Arabidopsis hypocotyl growth tends to be more responsive to $KAR_2$ [4, 39]. We examined if the preference towards a specific KAR molecule is also observed with KAI2 from other species. To this end, we used a line resulting from a cross of the *kai2* mutant *htl-2* with an Arabidopsis line transgenic for the cDNA of the rice *D14L*/*KAI2* [11], and tested its response to the two KAR molecules. In

contrast to *LjKAI2b*, *OsD14L/KAI2* mediated a stronger response to $KAR_2$ than to $KAR_1$ (Fig. 3c). This suggests that differential responsiveness of transgenic Arabidopsis lines to different karrikin species is caused by the specific amino acid sequence of the transgenic receptor and does not results from a general incompatibility of a heterologous KAI2 protein with the Arabidopsis background. Together, these results imply that LjKAI2a and LjKAI2b differ in their affinities to $KAR_1$ and $KAR_2$ or their possible breakdown products [30].

Besides karrikins also the stereoisomers of the synthetic strigolactone *rac*-GR24, $GR24^{5DS}$ and $GR24^{ent\text{-}5DS}$ trigger developmental responses via KAI2 as well as in Arabidopsis [10, 40]. To confirm the divergent responses mediated by LjKAI2a and LjKAI2b with yet another ligand we complemented the *Arabidopsis thaliana d14-1 kai2-2* double mutant with *LjKAI2a* and *LjKAI2b* and tested the hypocotyl response to these two GR24 stereoisomers (Fig. 3d). Lines expressing *LjKAI2a* responded to both with reduced hypocotyl elongation and a much stronger response to $GR24^{ent\text{-}5DS}$, whereas, interestingly, the lines expressing *LjKAI2b* did not significantly respond to any of the two stereoisomers. This contrasting sensitivity to GR24 stereoisomers together with the smaller differences in response to the KARs suggests that LjKAI2a and LjKAI2b differ in their binding pocket, resulting in divergent ligand binding specificity.

**Three amino acid residues at the binding pocket are decisive for ligand binding specificity**

To examine differences in binding specificity directly, we analysed the ligand binding of LjKAI2a and LjKAI2b *in vitro* by differential scanning fluorimetry (DSF) using purified recombinant proteins (Supplementary Fig. S4). This assay has been successfully used to characterize ligand binding to D14 and KAI2 proteins *in vitro* [21, 30]. Binding of $KAR_1$ and

$KAR_2$ to KAI2 could not be shown with this assay, possibly because karrikins are metabolised *in planta* and their metabolic products, not the molecules themselves, bind to the receptor *in vivo* [30]. However, the GR24 stereoisomers $GR24^{5DS}$ and $GR24^{ent\text{-}5DS}$ are functional and used sucessfully in DSF assays, where $GR24^{ent\text{-}5DS}$ triggers thermal destabilisation of KAI2 proteins from Arabidopsis, *Selaginella moellendorfii* and *Marchantia polymorpha* [30]. Here, $GR24^{ent\text{-}5DS}$ induced a thermal destabilization of LjKAI2a at a concentration > 50 µM but it did not cause any significant thermal shift of LjKAI2b (Fig. 4b).

To determine, which residues could be responsible for differential ligand binding we compared the protein sequences of KAI2a and KAI2b in legumes. This revealed conserved differences between the KAI2a and the KAI2b clade for 16 amino acids (Supplementary Fig. S5). However, four of these (KAI2a: Y157L, I188T, M223V; and KAI2b: I119V) are not conserved in *L. japonicus*. We wondered whether the remaining divergent amino-acids could be responsible for the observed differential binding and hypocotyl growth responses mediated by LjKAI2a and LjKAI2b. We used Arabidopsis KAI2 and rice D14L as additional filters because their response pattern to $KAR_1$ and $KAR_2$ in the Arabidopsis background was similar to LjKAi2a. Thus, we focussed on the amino acids conserved within the KAI2b clade, which differed from the KAI2a clade as well as from AtKAI2 and OsD14L/KAI2, namely T103, M161, L191, A226. We modelled LjKAI2a and LjKAI2b on the $KAR_1$-bound AtKAI2 crystal structure (4JYM) [5], and determined that only M161 (L160 in LjKAI2a) and L191 (S190 in LjKAI2a) are at the entrance or inside the pocket, respectively (Fig. 4a). In addition, we found that inside the pocket a highly conserved phenylalanine is exchanged for tryptophan at position 158 in LjKAI2b. Although

this tryptophan is not conserved among other LjKAI2b versions of the investigated legumes, we predicted that this bulky residue may have a strong impact on ligand binding. To understand whether these three residues are involved in determining the ligand binding specificity we mutated the receptor genes to swap the divergent amino acids (Fig. 4b). Swapping only the two amino acids that are conserved in legumes already strongly affected the thermal shift in response to GR24$^{ent\text{-}5DS}$ in the DSF assay. LjKAI2a$^{M160,L190}$ became much less responsive relative to LjKAI2a and displayed a slight thermal shift only with 200 µM GR24$^{ent\text{-}5DS}$, whereas LjKAI2b$^{L161,S191}$ gained the ability to respond to GR24$^{ent\text{-}5DS}$ at 200 µM. The changes in ligand-induced thermal shift were even more drastic when all three amino acids were swapped: LjKAI2a$^{M160,L190,W157}$ did not display any thermal shift in presence of GR24$^{ent\text{-}5DS}$, whereas LjKAI2b$^{L161,S191,F158}$ gained a response to GR24$^{ent\text{-}5DS}$ and displayed a thermal shift with ligand concentrations as low as 25 µM. In effect, the thermal shift response of LjKAI2a to GR24$^{ent\text{-}5DS}$ could be recapitulated by changing just three amino acids of LjKAI2b, and vice-versa. We conclude that residues L160/M161, S190/L191 and W158/F159 all contribute to the response of LjKAI2 proteins to GR24$^{ent\text{-}5DS}$.

To examine whether these three amino acid residues also determine ligand discrimination *in planta*, we transformed Arabidopsis *d14 kai2* double mutants with the mutated *LjKAI2a* and *LjKAI2b* genes driven by the Arabidopsis *KAI2* promoter and performed the hypocotyl growth assay in the presence of GR24$^{ent\text{-}5DS}$. Swapping only the two amino acids conserved in legumes (M160/L161 and S190/L191) was insufficient to exchange the ability between LjKAI2a and LjKAI2b to mediate hypocotyl responses to GR24$^{ent\text{-}5DS}$. However, swapping all three amino acids negatively affected the capacity of LjKAI2a$^{M160,L190,W157}$ to mediate a hypocotyl response to GR24$^{ent\text{-}5DS}$ whereas it

reconstituted a response via LjKAI2b$^{L161,S191,F158}$ in three independent transgenic lines (Fig. 5a and 5b). Together these results indicate that these three residues determine the difference in ligand binding preference between the two *L. japonicus* karrikin receptors KAI2a and KAI2b. Although $KAR_1$, $KAR_2$ and GR24$^{ent\text{-}5DS}$ are not the natural ligands of *L. japonicus* karrikin receptors, the evolution of different residues in the binding pocket of the duplicated KAI2 receptors suggest different functions for LjKAI2a and LjKAI2b.

**Identification of *L. japonicus* karrikin and strigolactone receptor mutants**

To explore the roles of *LjKAI2a* and *LjKAI2b* in *L. japonicus*, we searched for mutants in these genes as well as in *D14* and *MAX2*. We identified *LORE1* retrotransposon insertions in *L. japonicus KAI2a*, *KAI2b* and *MAX2* (*kai2a-1, kai2b-3*, *max2-1, max2-2, max2-3, max2-4*) [35, 41] and nonsense mutations in *D14* and *KAI2b* (*d14-1, kai2b-1, kai2b-2*) by TILLING [34] (Fig. 6a, Supplementary Table S1). Since some of the *max2* and *kai2b* mutants had problems with seed germination or production (Supplementary Table S1) we continued working with *kai2b-1, kai2b-3, max2-3, max2-4.* Quantitative RT-PCR analysis revealed that all mutations lead to a reduced transcript accumulation of the mutated genes in roots of the mutants except for *d14-1* (Supplementary Fig. S6a and S6b). Furthermore, the transcript accumulation of *LjKAI2a* and *LjKAI2b* was not affected by mutation of the respective other paralog (Supplementary Fig. S6a).

The LORE1 insertion in the *kai2a-1* mutant is located close (19 bp) to a splice acceptor site. Since some *LjKAI2a* transcript accumulated in the mutant, we sequenced this residual transcript to examine the possibility that a functional protein could still be made through loss of LORE1 by splicing. We found that indeed a transcript from ATG to stop accumulates in *kai2a-1* but it suffers from mis-splicing leading to a loss of the LORE1

transposon plus 15 bp (from 369 - 383), corresponding to five amino acids (YLNDV) at position 124-128 of the protein (Supplementary Fig. S7a and S7b). This amino-acid stretch reaches from a loop at the surface of the protein into the cavity of the binding pocket (Supplementary Fig. S7c). The artificial splice variant did not rescue the Arabidopsis *kai2-2* hypocotyl phenotype, confirming that it is not functional *in planta* and that the amino acids 124-YLNDV-128 are essential for *Lj*KAI2a function (Supplementary Fig. S7d).

**Karrikin treatment causes reduction in hypocotyl growth of *L. japonicus* in a *LjKAI2a*-dependent manner**

Phenotypically, *d14-1* and all allelic *max2* mutants of *L. japonicus* displayed increased shoot branching, indicating that the *L. japonicus* strigolactone receptor components D14 and MAX2 are involved in shoot branching inhibition (Fig. 6b and 6c), similar as in Arabidopsis, pea and rice [4, 38, 42, 43]. In contrast, we could not observe the canonical elongated hypocotyl phenotype, which is observed for Arabidopsis *kai2* mutants (and for mesocotyl in rice *d14l*/*kai2* mutants) in white light conditions [4, 11], neither for *L. japonicus* *kai2a* and *kai2b* single mutants nor for *kai2a-1 kai2b-1* double mutant or *max2* mutants. If anything the *kai2a-1 kai2b-1* and *max2* mutant hypocotyls were shorter than those of the wild type (Fig. 6d). This indicates that the requirement of KL perception for suppression of hypocotyl elongation under white light is not conserved in *L. japonicus* or that KL may not be produced under these conditions.

To examine whether *L. japonicus* hypocotyls are responsive to karrikin treatment, we measured the dose-response of hypocotyl elongation in wild-type to $KAR_1$, $KAR_2$ and also to *rac*-GR24. Hypocotyl elongation of wild type plants was progressively inhibited with

increasing concentrations of all three compounds (Fig. 7a). However, it was not suppressed by $KAR_1$ or $KAR_2$ treatment in the *kai2a-1 kai2b-1* double mutant and the *max2-4* mutant (Fig. 7b, Supplementary Fig. S8). This demonstrates that similar to Arabidopsis, the hypocotyl response to karrikin of *L. japonicus* depends on the KAI2-MAX2 receptor complex. We also examined the $KAR_1$ response of *kai2a* and *kai2b* single mutant hypocotyls and found that *kai2a-1* did not significantly respond to $KAR_1$ and $KAR_2$, while the two allelic *kai2b* mutants showed reduced hypocotyl growth in response to both karrikins (Fig. 7b). The transcript accumulation pattern of *DLK2* (*Lj2g3v0765370*) - which in Arabidopsis responds to karrikin in a *KAI2*-dependent fashion [4, 40] – was consistent with this observation: *DLK2* was induced in hypocotyls by $KAR_1$ and $KAR_2$ in a manner dependent on *LjKAI2a* but not *LjKAI2b* (Fig. 7c). Furthermore, *DLK2* expression was already lower in mock-treated *kai2a* hypocotyls than in mock-treated wild-type and *kai2b-3* hypocotyls (Supplementary Fig. S8b), indicating that in hypocotyls the endogenous KL ligand is perceived only by LjKAI2a and not by LjKAI2b. *rac*-GR24 treatment induced an increase of *DLK2* transcript in a partially *LjKAI2a*-dependent, *LjKAI2b*-independent and fully *MAX2*-dependent manner, suggesting that this induction is likely mediated via LjKAI2a and LjD14, similar as in Arabidopsis [4] (Fig. 7c). In summary, *LjKAI2a* appears to be necessary and sufficient to perceive karrikins in the hypocotyl via MAX2, possibly because expression of *LjKAI2b* in hypocotyls is too low under short day conditions (Supplementary Fig. S2b).

### *L. japonicus* root system architecture is modulated by $KAR_1$ but not by $KAR_2$ treatment

It was previously suggested that strigolactone signalling is involved in modulating root development of Arabidopsis and *Medicago truncatula* and that *rac*-GR24 treatment can trigger root system architecture changes in both species [44, 45, 46]. We examined whether *L. japonicus* root systems would respond to *rac*-GR24 as well as to $KAR_1$ and $KAR_2$ (Fig. 8a). Surprisingly, in contrast to Arabidopsis and *M. truncatula*, *L. japonicus* root systems responded neither to *rac*-GR24 nor to $KAR_2$. Only $KAR_1$ treatment lead to a dose-dependent decrease in primary root length and an increase of post-embryonic root (PER) number and thus, to a higher PER density (Fig. 8a). PERs include lateral and adventitious roots that are difficult to distinguish in *L. japonicus* seedlings. The instability of *rac*-GR24 over time in the medium could potentially prevent a developmental response of the root to this compound in our experiments [47]. However, refreshing the medium with new *rac*-GR24 or karrikins at 5 days post- germination, did not alter the outcome: PER density remained unaffected by $KAR_2$ and by rac-GR24 treatment (Supplementary Fig. S9). Consistently, we observed *DLK2* induction in roots after $KAR_1$ but not after $KAR_2$ treatment (Fig. 8b).

Together with the *L. japonicus* hypocotyl responses to $KAR_1$, $KAR_2$ and *rac*-GR24 this indicates organ-specific sensitivity or responsiveness to treatment with three compounds in *L. japonicus* and a more stringent uptake, perception and/or response system in the root.

Surprisingly, we found that roots responded to *rac*-GR24 treatment with increased *DLK2* transcript accumulation (Fig. 8c) although no change in root architecture was observed under this condition (Fig. 8a). To confirm the contrasting responses of *L. japonicus* root systems to $KAR_1$ and *rac*-GR24, and to test whether they result from divergent molecular signalling outputs that are independent from *DLK2* expression, we examined early

transcriptional responses after one, two and six hours' treatment of *L. japonicus* wild-type roots with $KAR_1$ and *rac*-GR24 using microarrays. Statistical analysis revealed a total number of 629 differentially expressed (DE) genes for $KAR_1$-treated and 232 genes for *rac*-GR24-treated roots (Supplementary Table S2). In agreement with previous reports from Arabidopsis and tomato [39, 48, 49] the magnitude of differential expression was low. Most of the DE genes upon $KAR_1$ and *rac*-GR24 treatment responded solely after 2h (Supplementary Fig. S10). Interestingly, only a minority of 48 genes responded in the same direction in response to both $KAR_1$ and *rac*-GR24, while the majority of genes responded specifically to $KAR_1$ (580 DEGs) or *rac*-GR24 (169 DEGs). In summary, the microarray experiment confirmed that *L. japonicus* roots respond to $KAR_1$ and *rac*-GR24 in a mainly distinct manner.

**Both LjKAI2a and LjKAI2b mediate root architecture-responses to KAR1**

To inspect which α/β-hydrolase receptor mediates the changes in *L. japonicus* root system architecture in response to $KAR_1$ treatment, we examined PER density in the karrikin receptor mutants. The *Ljkai2a-1 kai2b-1* double mutant and the *max2-4* mutant did not respond to $KAR_1$ treatment with changes in root system architecture (Fig. 9a, Supplementary Fig. S11). With 1 µM $KAR_1$ we obtained contradictory results for the single *kai2a* and *kai2b* mutants in independent experiments (Supplementary Fig. S11a and S11c). However, *kai2a* and *kai2b* single mutants but not the *kai2a kai2b* double mutant responded to a slightly higher concentration of 3 µM $KAR_1$ (Fig. 9a, Supplementary Fig. S12), indicating that LjKAI2a and LjKAI2b redundantly perceive $KAR_1$ (or a metabolite thereof) in *L. japonicus* roots. This pattern was mirrored by *DLK2* expression in roots: both *kai2a* and *kai2b* single mutants responded to $KAR_1$ with increased *DLK2* expression, while

the *kai2a-1 ka2b-1* double mutant and the *max2-4* mutant did not respond (Fig. 9b). In summary, we conclude that LjKAI2a and LjKAI2b act redundantly in roots in mediating the responses to $KAR_1$.

## Discussion

We found that the karrikin receptor gene *KAI2* has duplicated in legumes possibly during duplication of the whole genome that occurred in the Papilionoidaea before the diversification of legumes 59 million years ago [50]. In the model legume *L. japonicus*, the paralogs *KAI2a* and *KAI2b* remained functional since both mediate developmental responses to KARs and each can restore hypocotyl growth inhibition in an Arabidopsis *kai2* mutant. We also found two genes encoding the F-box protein MAX2. However, one of them underwent pseudogenization, leaving a single active protein in *L. japonicus* to deliver its responses to KARs. Gene duplication followed by sub- or neofunctionalization is an important driver in the evolution of complex signalling networks and signalling specificities. We provide evidence that *L. japonicus* KAI2a and KAI2b diversified in their ligand-binding specificity as well as organ-specific function.

$KAR_1$ and $KAR_2$ are highly similar compounds that differ only by one additional methyl group in $KAR_1$. Nevertheless, LjKAI2a and LjKAI2b differ in their sensitivity to these compounds, since in the Arabidopsis hypocotyl assay, LjKAI2a mediates an equal response to $KAR_1$ and $KAR_2$, while LjKAI2b confers a stronger response to $KAR_1$ than to $KAR_2$ (Fig. 10b). Thereby, LjKAI2b changes the response preference of Arabidopsis, which usually responds more strongly to $KAR_2$ [2, 39, this work]. GR24$^{ent\text{-}5DS}$, an enantiomer of the synthetic strigolactone analogue *rac*-GR24 has been shown genetically to act via Arabidopsis KAI2 and to bind to KAI2 *in vitro* [30, 40]. LjKAI2a also mediates strong

Arabidopsis hypocotyl growth responses to GR24$^{ent\text{-}5DS}$ but this is not the case for LjKAI2b. Furthermore, LjKAI2b may be less sensitive to the endogenous ligand of Arabidopsis KAI2, since its ability to restore hypocotyl growth inhibition in untreated Arabidopsis is slightly decreased as compared to LjKAI2a. Together, these results demonstrate that the α/β-fold hydrolase receptor is sufficient to explain ligand sensitivity in the Arabidopsis hypocotyl assay. The differential sensitivity of LjKAI2a and LjKAI2b to GR24$^{ent\text{-}5DS}$ was confirmed *in vitro* by DSF assay: GR24$^{ent\text{-}5DS}$ induced a thermal shift of LjKAI2a but did not induce thermal destabilization of LjKAI2b.

Identifying the determinants of ligand-binding specificity of D14 and different KAI2 proteins is an area of active research. Although some factors such as geometry and rigidity of the binding pocket have been proposed to determine specificity of KAI2-like proteins for strigolactones vs. karrikins in *Physcomitrella patens* and in parasitic weeds [31, 32], it is unclear how differential binding preference for very similar molecules is achieved. We identified three amino acids at the ligand-binding pocket that differ between LjKAI2a and LjKAI2b and explain ligand response to GR24$^{ent\text{-}5DS}$.Two of these amino acids are conserved across the legume KAI2a and KAI2b clades, namely L160 and S190 in KAI2a and M161 and L191 in LjKAI2b. An exchange of these two amino acids was sufficient to strongly reduce sensitivity of LjKAI2a to GR24$^{ent\text{-}5DS}$ in the DSF assay and to gain a thermal shift of LjKAI2b. Neither amino acid change is predicted to substantially impact the pocket volume or geometry but the amino acids of LjKAI2b are more hydrophobic, which may explain the repulsion of the more hydrophilic GR24$^{ent\text{-}5DS}$ and also the preference for the more hydrophobic $KAR_1$ over $KAR_2$. A similar phenomenon was observed in *Brassica tournefortii*, a fire-following weed that has three *KAI2* genes, of which KAI2c does not seem to be functional [51]. Similar to the situation in *L. japonicus*, BtKAI2b

mediated a greater sensitivity to $KAR_1$ over $KAR_2$ in the Arabidopsis background, while it was the reverse for BtKAI2a. Again, this was explained by two amino acid changes in the binding pocket between LjKAI2a and LjKAI2b towards more hydrophobic amino acids (V98L, V191L). Notably, one of these residues in *B. tournefortii* (V98L) is in a different position than the specificity- determining residue 160/161 in *L. japonicus* KAI2a/KAI2b. This suggests that these receptors are highly plastic and that similar binding-specificities may be achieved by changing hydrophobicity in different positions of the pocket. Furthermore, the position of the change towards stronger hydrophobicity may be involved in conferring sensitivity to the ligand, as *B. tournefortii* KAI2 proteins respond to lower ligand concentrations than *L. japonicus* KAI2 proteins in the DSF assay [51, this work].

Exchanging L160/M161 and S190/L191 between *L. japonicus* KAI2a and KAI2b was sufficient to change their sensitivity to GR24$^{ent\text{-}5DS}$ in the DSF *in vitro* assay. However, the developmental response of Arabidopsis hypocotyls was hardly changed, possibly because *in vivo*, suboptimal ligand binding to the receptor can be stabilized by interacting proteins. A third amino acid difference (F157/W158) between the two KAI2 proteins occurs in *L. japonicus*. This residue strongly determines sensitivity to GR24$^{ent\text{-}5DS}$ likely because in addition to increased hydrophobicity of tryptophan vs. phenylalanine the bulky tryptophan in the pocket of KAI2b may sterically hinder GR24$^{ent\text{-}5DS}$ binding. However, it still allows sensitivity to $KAR_1$, which is larger than $KAR_2$. When all three amino acids are exchanged, LjKAI2a completely loses GR24$^{ent\text{-}5DS}$ - responsiveness *in vitro* as well as in the Arabidopsis hypocotyl assay whereas LjKAI2b gains full responsiveness.

*B. tournefortii* is a fire-following plant, whose seeds respond to karrikins by breaking dormancy and germinating [51]. Therefore, it makes adaptive sense for *B. tournefortii* to maintain two copies of KAI2, one of which is specialized for $KAR_1$, the most abundant

KAR in smoke, and the other of which may be specialized for the endogenously produced ligand. However, for *L. japonicus*, which is not a fire-follower, $KAR_1$, $KAR_2$ and $GR24^{ent\text{-}5DS}$ are likely not natural KAI2 ligands. Nevertheless, the maintenance of two *KAI2* genes in the legumes, each with amino acid polymorphisms confering differences in binding preferences to artificial ligands, requires an adaptive basis. One possibility is that *L. japonicus* KAI2a and KAI2b have specialized to bind different ligands *in planta* and that legumes may produce at least two different versions of the as-yet-unknown KL compound. The distinct expression patterns and developmental roles of LjKAI2a and LjKAI2b might also be consistent with tissue-specific ligands, or even an endogenous ligand versus an exogenous ligand derived from the rhizosphere. From our assays with artificial ligands we extrapolate that KAI2b is likely more stringent regarding the ligand's chemical properties. The additional amino acid change that has occurred in *L. japonicus* but not in the other examined legumes may indicate that the KL bouquet of *L. japonicus* has further diversified. Once the identity of KL and its putative different versions have been identified it will be interesting to investigate the biological significance of this receptor sub-functionalization and the putative diversity of their ligands.

Using *kai2a* and *kai2b* mutants of *L. japonicus*, we determined that LjKAI2a alone mediates developmental and transcriptional responses to exogenously-applied karrikins in hypocotyls, whereas both LjKAI2a and LjKAI2b act in roots (Fig. 10a). In addition, we found that *L. japonicus* root systems respond to karrikin treatment with slightly increased postembryonic root (PER) density (higher PER number and shorter primary roots). Surprisingly, this occurred exclusively in response to $KAR_1$, while in contrast, hypocotyl growth inhibition was achieved with $KAR_1$, $KAR_2$ and *rac*-GR24 (Fig. 10a). To our

knowledge such an organ-specific discrimination of different but very similar KAR molecules has not previously been so clearly observed. However, a similar scenario could be at play in rice, in which a transcriptome analysis of $KAR_2$-treated rice roots found no differentially expressed genes, whereas rice mesocotyls responded with growth inhibition to the same treatment [11]. Previous work suggested that KARs are not directly bound by KAI2, but they may be metabolized first to yield the correct KAI2-ligand [30]. It is possible that the enzymes involved in KAR metabolism in hypocotyls and roots differ in their substrate specificities. This would imply that the single methyl group, which distinguishes $KAR_1$ from $KAR_2$, is sufficient to impede or otherwise impact upon specialized metabolism of karrikins. Alternatively, the transport of the $KAR_2$-derived metabolic product could be limited in the root system. Finally, $KAR_2$-derivatives may be specifically catabolised in roots thus limiting the response. Although $KAR_2$ fails to induce increased PER density and *DLK2* expression in *L. japonicus* roots, *rac*-GR24 is still able to trigger KAI2-dependent *DLK2* transcript accumulation albeit being unable to increase PER density. It is possible that DLK2 activation is mediated via D14, which may not be involved in regulating root architecture in *L. japonicus*. Alternatively, downstream events triggered by KAI2 might differ depending on the specific ligand.

In Arabidopsis, *kai2* and *max2* mutants display an increased lateral root density [10]. This is somewhat different to our observation that $KAR_1$ treatment triggers increased PER density in *L. japonicus*. The discrepancy may result from different physiological optima between the two species or from nutrient conditions in the two experimental systems. We observed the $KAR_1$ response of *L. japonicus* root systems in half-Hoagland solution with low phosphate levels (2.5µM $PO_4^{3-}$) and without sucrose, whereas the root assay in Arabidopsis was conducted in ATS medium (*Arabidopsis thaliana* salts) with 1% sucrose.

Phosphate and sucrose levels have previously been described to influence the effect of strigolactone and *rac*-GR24 on Arabidopsis root architecture [44, 52, 53].

In Arabidopsis and rice, KAI2/D14L is required to inhibit hypocotyl and mesocotyl elongation, respectively [3, 4, 11]. Since these two species are evolutionary distant from each other, but have both retained a function of KL signalling in inhibiting the growth of similar organs, it seemed likely that this function would be conserved among a large number of plant species. Surprisingly, in *L. japonicus*, we observed no elongated hypocotyl phenotype for the *kai2a-1 kai2b-1* double and two allelic *max2* mutants (Fig. 5). However, we could trigger a reduction of hypocotyl elongation by treatment with $KAR_1$, $KAR_2$ and *rac*-GR24 in the wild type and in a *LjKAI2a* and *LjMAX2*-dependent manner. Thus, it is possible that endogenous KL levels in *L. japonicus* hypocotyls are insufficient to cause inhibition of hypocotyl elongation, at least under our growth conditions.

In this work, we have demonstrated sub-functionalization of two KAI2 copies in *L. japonicus* with regard to their ligand-binding specificity - mediated by three amino acids in the binding-pocket - and organ-specific relevance. Furthermore, we find organ-specific responsiveness of *L. japonicus* to different artificial KAI2 ligands. Our present work suggests multiple endogenous ligands that can be discriminated by LjKAI2a and LjKAI2b. It opens novel research avenues towards understanding the diversity in KL ligand-receptor relationships and in developmental responses to both, as yet, unknown and synthetic butenolides that influence diverse aspects of plant development.

## Methods

### Plant material and seed germination

The *A. thaliana kai2-2* (Ler background) and *d14-1* (Col-0 background) mutants are from [4], the *d14-1 kai2-2* double mutant from [40], the *htl-2* mutant was provided by Min Ni [54] and the cross with K02821 is from [11]. Seeds were surface sterilized with 70% EtOH. For synchronizing the germination, seeds were placed on ½ MS 1% agar medium and maintained at 4°C in the dark for 72 hours.

The *L. japonicus* Gifu *max2-1, max2-2, max2-3, max2-4, kai2a-1* and *kai2b-3* mutations are caused by a LORE1 insertion. Segregating seed stocks for each insertion were obtained from the Lotus Base (https://lotus.au.dk, [55]) or Makoto Hayashi (NIAS, Tsukuba, Japan, [41] for *max2-2*. The *d14-1, kai2b-1* and *kai2b-2* mutants were obtained by TILLING [34] at RevGenUK (https://www.jic.ac.uk/technologies/genomic-services/revgenuk-tilling-reverse-genetics/). Homozygous mutants were identified by PCR using primers indicated in S3 Table. For germination, *L. japonicus* seeds were manually scarified with sand-paper and surface sterilized with 1% NaClO. Imbibed seeds were germinated on 1/2 Hoagland medium containing 2.5µM $PO_4^{3-}$ and 0.4% Gelrite (www.duchefa-biochemie.com), at 24°C for 3 days in the dark, or on ½ MS 0.8% agar at 4°C for 3 days in dark (only for the experiment in Fig. 6d).

**Protein sequence alignment, phylogenetic tree and synteny**

Protein sequences were retrieved using tBLASTn with *AtKAI2*, *AtDLK2* and *AtMAX2*, against the NCBI database, the plantGDB database and the *L. japonicus* genome V2.5 (http://www.kazusa.or.jp/lotus). The presence of MAX2-like was identified by tBLASTn in an in-house genome generated by next generation sequencing using CLC Main Workbench [56]. Pea sequences were found by BLASTn on “pisum sativum v2” database with AtKAI2 as query (https://www.coolseasonfoodlegume.org). The MAFFT alignment

(https://mafft.cbrc.jp) of the protein sequences was used to generate Maximum-likelihood tree with 1000 bootstrap replicates in MEGA7 [57]. For the synteny analysis of *MAX2* and *MAX2-like*, flanking sequences were retrieved from the same in-house genome [56].

**Structural homology modelling of proteins**

Proteins were modelled using SWISS-MODEL tool (https://swissmodel.expasy.org) with the *A. thaliana* KAI2 (4JYM) templates [5].

**Bacterial protein expression and purification**

Full-length *L. japonicus* coding sequences were cloned into pE-SUMO Amp. Clones were sequence-verified and transformed into Rosetta DE3 pLysS cells (Novagen). Subsequent protein expression and purification were performed as described previously [30], with the following modifications: the lysis and column wash buffers contained 10 mM imidazole, and a cobalt-charged affinity resin was used (TALON, Takara Bio).

**Differential scanning fluorimetry**

DSF assays were performed as described previously [30]. Assays were performed in 384-well format on a Roche LightCycler 480 II with excitation 498 nm and emission 640 nm (SYPRO Tangerine dye peak excitation at 490 nm). Raw fluorescence values were transformed by calculating the first derivation of fluorescence over temperature. These data were then imported into GraphPad Prism 8.0 software for plotting. Data presented are the mean of three super-replicates from the same protein batch; each super-replicate comprised four technical replicates at each ligand concentration. Experiments were performed at least twice.

## Plasmid generation

Genes and promoter regions were amplified using Phusion PCR according to standard protocols and using primers indicated in Supplementary Table S3. Plasmids were constructed by Golden Gate cloning [58] as indicated in Supplementary Table S4.

## Plant transformation

*kai2-2* and *d14-1* mutants were transformed by floral dip in *Agrobacterium tumefaciens* AGL1 suspension. Transgenic seedlings were selected by mCherry fluorescence and resistance to 20 µg/mL hygromycin B in growth medium. Experiments were performed using T2 or T3 generations, with transformed plants validated by mCherry fluorescence.

## Shoot branching assay

*A. thaliana* and *L. japonicus* were grown for 4 and 7 weeks, respectively in soil in the greenhouse at 16h/8h light/dark cycles. Branches with length superior to 1cm were counted, and the height of each plant was measured.

## Hypocotyl elongation assay

*A. thaliana* were grown for 5 days on half-strength Murashige and Skoog (MS) medium containing 1% agar (BD). *L. japonicus* seedlings were grown for 6 days on half-strength Hoagland medium containing 2.5µM $PO_4^{3-}$ and 0.4% Gelrite (www.duchefa-biochemie.com), or on half-strength MS containing 0.8% agar (only for experiment in Fig. 6d). Long-day conditions with 16h/8h light/dark cycles were used to test restoration of hypocotyl growth suppression by cross-species complementation (Fig. 2a). For Karrikin,

*rac*-GR24, GR24$^{5DS}$ and GR24$^{ent\text{-}5DS}$ treatments the medium was supplied with $KAR_1$ (www.olchemim.cz), $KAR_2$ (www.olchemim.cz), *rac*-GR24 (www.chiralix.com) GR24$^{5DS}$ and GR24$^{ent\text{-}5DS}$ (www.strigolab.eu) or equal amounts of the corresponding solvent as a control. Karrikins were solubilized in 75% methanol and *rac*-GR24 and the GR24 stereoisomers in 100% acetone, at 10mM stock solution. Short-day conditions at 8h/16h light/dark cycles were used to test hormone responsiveness. After high-resolution scanning, the hypocotyl length was measured with Fiji (http://fiji.sc/).

**Root system architecture assay**

*L. japonicus* germinated seeds were transferred onto new plates containing $KAR_1$ (www.olchemim.cz), $KAR_2$ (www.olchemim.cz), *rac*-GR24 (www.chiralix.com) or the corresponding solvent. Karrikins were solubilized in 75% methanol and *rac*-GR24 in 100% acetone, at 10 mM stock solution. Plates were partially covered with black paper to keep the roots in the dark, and placed at 24°C with 16-h-light/8-h-dark cycles for 2 weeks. After high-resolution scanning, post-embryonic root number was counted and primary root length measured with Fiji (http://fiji.sc/).

**Treatment for analysis of transcript accumulation**

Seedling roots were placed in 1/2 Hoagland solution with 2.5µM $PO_4^{3-}$ containing 1 or 3 µM $Karrikin_1$ (www.olchemim.cz for qPCR analysis, synthesized according to [59] for microarray analysis), Karrikin2 (www.olchemim.cz), *rac*-GR24 (www.chiralix.com) or equal amounts of the corresponding solvents for the time indicated in Figure legends and the roots were covered with black paper to keep them in the dark.

## Microarray analysis

Three biological replicates were performed for each treatment. Root tissues were harvested, rapidly blotted dry and shock frozen in liquid nitrogen. RNA was extracted using the Spectrum Plant Total RNA Kit (www.sigmaaldrich.com). RNA was quantified and evaluated for purity using a Nanodrop Spectrophotometer ND-100 (NanoDrop Technologies, Willington, DE) and Bioanalyzer 2100 (Agilent, Santa Clara, CA). For each sample, 500 ng of total RNA was used for the expression analysis of each sample using the Affymetrix GeneChip® Lotus1a520343 (Affymetrix, Santa Clara, CA). Probe labeling, chip hybridization and scanning were performed according to the manufacturer's instructions for IVT Express Labeling Kit (Affymetrix). The Microarray raw data was normalized with the Robust Multiarray Averaging method (RMA) [60] using the Bioconductor [61] package "Methods for Affymetrix Oligonucleotide Arrays" (affy version 1.48.0) [62]. Control and rhizobial probesets were removed before statistical analysis. Differential gene expression was analyzed with the Bioconductor package "Linear Models for Microarray Data" (LIMMA version 3.26.8) [63]. The package uses linear models for parameter estimation and an empirical Bayes method for differential gene expression assessment [64]. P-values were adjusted due to multiple comparisons with the Benjamini-Hochberg correction (implemented in the LIMMA package). Probesets were termed as significantly differentially expressed, if their adjusted p-value was smaller than or equal to 0.01 and the fold change for at least one contrast showed a difference of at least 50%. To identify the corresponding gene models, the probeset sequences were used in a BLAST search against *L. japonicus* version 2.5 CDS and version 3.0 cDNA sequences (http://www.kazusa.or.jp/lotus/). If, based on the bitscore, multiple identical hits were found, we took the top hit in version 2.5 CDS as gene corresponding to the probe. For

version 3.0 cDNA search we used the best hit, that was not located on chromosome 0, if possible. For probesets known to target chloroplast genes (probeset ID starting with Lj_), we preferred the best hit located on the chloroplast chromosome, if possible. Probeset descriptions are based on the info file of the *L. japonicus* Microarray chip provided by the manufacturer (Affymetrix).

### qPCR analysis

Tissue harvest, RNA extraction, cDNA synthesis and qPCR were performed as described previously [56]. qPCR reactions were run on an iCycler (Biorad, www.bio-rad.com) or on QuantStudio5 (applied biosystem, www.thermofisher.com). Expression values were calculated according to the ΔΔCt method [65]. Expression values were normalized to the expression level of the housekeeping gene *Ubiquitin*. For each condition three to four biological replicates were performed. Primers are indicated in Supplementary Table S3.

### Statistics

Statistical analyses were performed using Rstudio (www.rstudio.com) after log transformation for qPCR analysis. F- and p-values for all figures are provided in Supplementary Table S5.

## Acknowledgments

We are grateful to Andreas Keymer and Priya Pimprikar for cDNAs from root, flower, leaf and stem; and to Verena Klingl for excellent technical support; to Martin Parniske (LMU Munich, Germany) for providing microarray chips and for setting up the *L. japonicus* mutant collection at the Sainsbury laboratory Norwich; to Jens Stougaard and all scientists

at LotusBase for the LORE1 insertion lines; and to David Nelson (University of California Riverside, USA) for fruitful discussion. We thank Min Ni (University of Minnesota, USA) for seeds of the *A. thaliana htl-2* mutant. The study was supported by an Australian Research Council Future Fellowship (FT150100162) to M.T.W. and the Emmy Noether program of the DFG, grant GU1423/1-1 to C.G..

## Author contributions

S.C. performed most experiments, S.T. contributed Supplementary Fig. S7 and the Arabidopsis lines and images of Arabidopsis hypocotyls for Fig. 5, M.G. performed computational micro-array data analysis, E.B. contributed Supplementary Fig. S3, S.B. contributed Fig. 6b and 6c, V.B. performed preliminary experiments to examine the *L. japonicus* hypocotyl response to karrikins, M.S. synthesized KAR1, T.L.W. contributed *kai2b-1* and *d14-1* EMS mutants by TILLING, Y.T. and M.U. performed microarray hybridization, M.T.W. performed protein purification and DSF assays. S.C. and C.G. designed research and wrote the manuscript. All authors commented on the manuscript. C.G. supervised the study and acquired funding.

## References

1. Flematti GR, Ghisalberti EL, Dixon KW, Trengove RD. A compound from smoke that promotes seed germination. *Science* **305**, 977 (2004).

2. Nelson DC*, et al.* Karrikins discovered in smoke trigger Arabidopsis seed germination by a mechanism requiring gibberellic acid synthesis and light. *Plant Physiol* **149**, 863-873 (2009).

3. Nelson DC*, et al.* F-box protein MAX2 has dual roles in karrikin and strigolactone signaling in *Arabidopsis thaliana*. *Proc Natl Acad Sci U S A* **108**, 8897-8902 (2011).

4. Waters MT*, et al.* Specialisation within the DWARF14 protein family confers distinct responses to karrikins and strigolactones in Arabidopsis. *Development* **139**, 1285-1295 (2012).

5. Guo Y, Zheng Z, La Clair JJ, Chory J, Noel JP. Smoke-derived karrikin perception by the α/β-hydrolase KAI2 from Arabidopsis. *Proc Natl Acad Sci U S A* **110**, 8284-8289 (2013).

6. Kagiyama M*, et al.* Structures of D14 and D14L in the strigolactone and karrikin signaling pathways. *Genes Cells* **18**, 147-160 (2013).

7. Conn CE, Nelson DC. Evidence that KARRIKIN-INSENSITIVE2 (KAI2) receptors may perceive an unknown signal that is not karrikin or strigolactone. *Front Plant Sci* **6**, 1219 (2016).

8. Li W*, et al.* The karrikin receptor KAI2 promotes drought resistance in *Arabidopsis thaliana*. *PLoS Genet* **13**, e1007076 (2017).

9. Swarbreck SM, Guerringue Y, Matthus E, Jamieson FJC, Davies JM. Impairment in karrikin but not strigolactone sensing enhances root skewing in *Arabidopsis thaliana*. *Plant J*, 607-621 (2019).

10. Villaecija Aguilar JA*, et al. SMAX1/SMXL2* regulate root and root hair development downstream of KAI2-mediated signalling in Arabidopsis. *PLoS Genet* **15**, 1-27 (2019).

11. Gutjahr C*, et al.* Rice perception of symbiotic arbuscular mycorrhizal fungi requires the karrikin receptor complex. *Science* **350**, 1521-1524 (2015).

12. Sun YK, Flematti GR, Smith SM, Waters MT. Reporter gene-facilitated detection of compounds in Arabidopsis leaf extracts that activate the karrikin signaling pathway. *Front Plant Sci* **7**, 1799 (2016).

13. Hrdlička J*, et al.* Quantification of karrikins in smoke water using ultra-high performance liquid chromatography–tandem mass spectrometry. *Plant Methods* **15**, 81 (2019).

14. Nelson DC, Flematti GR, Ghisalberti EL, Dixon KW, Smith SM. Regulation of seed germination and seedling growth by chemical signals from burning vegetation. *Annu Rev Plant Biol* **63**, 107-130 (2012).

15. Cook CE, Whichard LP, Turner B, Wall ME, Egley GH. Germination of witchweed (*Striga lutea* Lour.): isolation and properties of a potent stimulant. *Science* **154**, 1189-1190 (1966).

16. Akiyama K, Matsuzaki K, Hayashi H. Plant sesquiterpenes induce hyphal branching in arbuscular mycorrhizal fungi. *Nature* **435**, 824-827 (2005).

17. Gomez-Roldan V*, et al.* Strigolactone inhibition of shoot branching. *Nature* **455**, 189-194 (2008).

18. Umehara M*, et al.* Inhibition of shoot branching by new terpenoid plant hormones. *Nature* **455**, 195-200 (2008).

19. Al-Babili S, Bouwmeester HJ. Strigolactones, a novel carotenoid-derived plant hormone. *Annu Rev Plant Biol* **66**, 161-186 (2015).

20. Matthys C*, et al.* The Whats, the Wheres and the Hows of strigolactone action in the roots. *Planta* **243**, 1327-1337 (2016).

21. Hamiaux C*, et al.* DAD2 is an alpha/beta hydrolase likely to be involved in the perception of the plant branching hormone, strigolactone. *Curr Biol* **22**, 2032-2036 (2012).

22. Toh S, Holbrook-Smith D, Stokes ME, Tsuchiya Y, McCourt P. Detection of parasitic plant suicide germination compounds using a high-Throughput Arabidopsis HTL/KAI2 strigolactone perception system. *Chem & Biol* **21**, 1253 (2014).

23. Stanga JP, Smith SM, Briggs WR, Nelson DC. *SUPPRESSOR OF MORE AXILLARY GROWTH2 1* controls seed germination and seedling development in Arabidopsis. *Plant Physiol* **163**, 318-330 (2013).

24. Zhou F*, et al.* D14-SCF(D3)-dependent degradation of D53 regulates strigolactone signalling. *Nature* **504**, 406-410 (2013).

25. Jiang L*, et al.* DWARF 53 acts as a repressor of strigolactone signalling in rice. *Nature* **504**, 401-405 (2013).

26. Soundappan I*, et al.* SMAX1-LIKE/D53 family members enable distinct MAX2-dependent responses to strigolactones and karrikins in Arabidopsis. *Plant Cell* **27**, 3143-3159 (2015).

27. Wang L*, et al.* Strigolactone signaling in Arabidopsis regulates shoot development by targeting D53-Like SMXL repressor proteins for ubiquitination and degradation. *Plant Cell* **27**, 3128-3142 (2015).

28. Bythell-Douglas R*, et al.* Evolution of strigolactone receptors by gradual neo-functionalization of KAI2 paralogues. *BMC Biol* **15**, 52 (2017).

29. Végh A*, et al.* Comprehensive analysis of *DWARF14-LIKE2* (*DLK2*) reveals its functional divergence from strigolactone-related paralogs. *Front Plant Sci* **8**, 1-14 (2017).

30. Waters MT, Scaffidi A, Moulin SL, Sun YK, Flematti GR, Smith SM. A *Selaginella moellendorffii* ortholog of KARRIKIN INSENSITIVE2 functions in Arabidopsis development

but cannot mediate responses to karrikins or strigolactones. *Plant Cell* **27**, 1925-1944 (2015).

31. Bürger M*, et al.* Structural basis of karrikin and non-natural strigolactone perception in *Physcomitrella patens*. *Cell Reports* **26**, 855-865 (2019).

32. Conn CE*, et al.* Convergent evolution of strigolactone perception enabled host detection in parasitic plants. *Science* **349**, 540-543 (2015).

33. Toh S*, et al.* Structure-function analysis identifies highly sensitive strigolactone receptors in Striga. *Science* **350**, 203-207 (2015).

34. Perry JA*, et al.* A TILLING reverse genetics tool and a web-accessible collection of mutants of the legume *Lotus japonicus*. *Plant Physiol* **131**, 866-871 (2003).

35. Malolepszy A*, et al.* The *LORE1* insertion mutant resource. *Plant J* **88**, 306-317 (2016).

36. Wojciechowski MF, Lavin M, Sanderson MJ. A phylogeny of legumes (Leguminosae) based on analysis of the plastid *matK* gene resolves many well-supported subclades within the family. *American J Bot* **91**, 1846-1862 (2004).

37. Shen H, Luong P, Huq E. The F-box protein MAX2 functions as a positive regulator of photomorphogenesis in Arabidopsis. *Plant Physiol* **145**, 1471-1483 (2007).

38. Stirnberg P, Furner IJ, Ottoline Leyser HM. MAX2 participates in an SCF complex which acts locally at the node to suppress shoot branching. *Plant J* **50**, 80-94 (2007).

39. Nelson DC, Flematti GR, Riseborough JA, Ghisalberti EL, Dixon KW, Smith SM. Karrikins enhance light responses during germination and seedling development in *Arabidopsis thaliana*. *Proc Natl Acad Sci U S A* **107**, 7095-7100 (2010).

40. Scaffidi A*, et al.* Strigolactone hormones and their stereoisomers signal through two related receptor proteins to induce different physiological responses in Arabidopsis. *Plant Physiol* **165**, 1221-1232 (2014).

41. Fukai E*, et al.* Establishment of a *Lotus japonicus* gene tagging population using the exon-targeting endogenous retrotransposon LORE1. *Plant J* **69**, 720-730 (2012).

42. Beveridge CA, Ross JJ, Murfet IC. Branching in pea (action of genes *Rms3* and *Rms4*). *Plant physiol* **110**, 859-865 (1996).

43. Ishikawa S, Maekawa M, Arite T, Onishi K, Takamure I, Kyozuka J. Suppression of tiller bud activity in tillering dwarf mutants of rice. *Plant Cell Physiol* **46**, 79-86 (2005).

44. Ruyter-Spira C*, et al.* Physiological effects of the synthetic strigolactone analog GR24 on root system architecture in Arabidopsis: another belowground role for strigolactones? *Plant Physiol* **155**, 721-734 (2011).

45. Jiang L*, et al.* Strigolactones spatially influence lateral root development through the cytokinin signaling network. *J Exp Bot* **67**, 379-389 (2016).

46. De Cuyper C*, et al.* From lateral root density to nodule number, the strigolactone analogue GR24 shapes the root architecture of *Medicago truncatula*. *J Exp Bot* **66**, 137-146 (2015).

47. Halouzka R, Tarkowski P, Zwanenburg B, Cavar Zeljkovic S. Stability of strigolactone analog GR24 toward nucleophiles. *Pest Manag Sci* **74**, 896-904 (2018).

48. Mayzlish-Gati E*, et al.* Strigolactones are positive regulators of light-harvesting genes in tomato. *J Exp Bot* **61**, 3129-3136 (2010).

49. Mashiguchi K*, et al.* Feedback-regulation of strigolactone biosynthetic genes and strigolactone-regulated genes in arabidopsis. *Biosci Biotechnol Biochem* **73**, 2460-2465 (2009).

50. Wong MML*, et al.* Novel insights into karyotype evolution and whole genome duplications in legumes. BioRxiv 099044 (2017).

51. Sun YK*, et al.* Divergent receptor proteins confer responses to different karrikins in two ephemeral weeds. BioRxiv 376939 (2019).

52. Mayzlish-Gati E*, et al.* Strigolactones are involved in root response to low phosphate conditions in Arabidopsis. *Plant Physiol* **160**, 1329-1341 (2012).

53. Madmon O*, et al.* Expression of *MAX2* under *SCARECROW* promoter enhances the strigolactone/MAX2 dependent response of Arabidopsis roots to low-phosphate conditions. *Planta* **243**, 1419-1427 (2016).

54. Sun X, Ni M. HYPOSENSITIVE TO LIGHT, an alpha/beta fold protein, acts downstream of ELONGATED HYPOCOTYL 5 to regulate seedling de-etiolation. *Mol Plant* **4**, 116-126 (2011).

55. Urbański DF, Małolepszy A, Stougaard J, Andersen SU. Genome-wide *LORE1* retrotransposon mutagenesis and high-throughput insertion detection in *Lotus japonicus*. *Plant J* **69**, 731-741 (2012).

56. Pimprikar P*, et al.* A CCaMK-CYCLOPS-DELLA complex activates transcription of *RAM1* to regulate arbuscule branching. *Curr Biol* **26**, 987-998 (2016).

57. Kumar S, Stecher G, Tamura K. MEGA7: Molecular Evolutionary Genetics Analysis version 7.0 for bigger datasets. *Mol Biol Evol* **33**, 1870-1874 (2016).

58. Binder A*, et al.* A modular plasmid assembly kit for multigene expression, gene silencing and silencing rescue in plants. *PLoS One* **9**, e88218 (2014).

59. Matsuo K, Shindo M. Efficient synthesis of karrikinolide via Cu(II)-catalyzed lactonization. *Tetrahedron* **67**, 971-975 (2011).

60. Irizarry RA*, et al.* Exploration, normalization, and summaries of high density oligonucleotides array probe level data. *Biostatistics* **4**, 249-264 (2003).

61. Gentleman RC*, et al.* Bioconductor: open software development for computational biology and bioinformatics. *Genome Biol* **5**, R80-R80 (2004).

62. Gautier L, Cope L, Bolstad BM, Irizarry RA. affy—analysis of Affymetrix GeneChip data at the probe level. *Bioinfo* **20**, 307-315 (2004).

63. Smyth GK. limma: Linear Models for Microarray Data. In: *Bioinformatics and computational biology solutions using R and Bioconductor* (eds Gentleman RC, Carey VJ, Huber W, Irizarry RA, Dudoit S). Springer New York (2005).

64. Smyth GK. Linear models and empirical bayes methods for assessing differential expression in microarray experiments. *Statist Appl Genet Mol Biol* **3**, 1-26 (2004).

65. Czechowski T, Bari RP, Stitt M, Scheible W, Udvardi MK. Real-time RT-PCR profiling of over 1400 Arabidopsis transcription factors: unprecedented sensitivity reveals novel root- and shoot-specific genes. *Plant J* **38**, 366-379 (2004).

## Figure legends

**Figure 1 | The KAI2 gene underwent duplication prior to diversification of the legumes.**

Phylogenetic tree of KAI2 and D14 rooted with bacterial RbsQ from indicated species (*Lj, Lotus japonicus; Gm, Glycine max; Ps, Pisum sativum; Mt, Medicago truncatula; At, Arabidopsis thaliana; Pt, Populus trichocarpa; Os, Oryza sativa; Zm, Zea mays; Sb, Sorghum bicolor; Mp, Marchantia polymorpha*). Protein sequences were aligned using MAFFT. MEGA7 was used to generate a tree inferred by Maximum Likelihood method. The tree with the highest log likelihood (-6038.38) is shown. The percentage of trees in

which the associated taxa clustered together is shown next to the branches. Values below 50 were ignored. *KAI2* duplication in the legumes is highlighted by red and blue branches.

**Figure 2 | *Lotus japonicus D14*, *KAI2a* and *KAI2b* can replace *D14* and *KAI2* in Arabidopsis, respectively.**

(**a**) Hypocotyl length of *A. thaliana* wild-type (L*er*), *kai2-2* and *kai2-2* lines complemented by *AtD14, AtKAI2, LjD14, LjKAI2a* and *LjKAI2b*, driven by the *AtKAI2* promoter at 6 days post germination (dpg). Seedlings were grown in 8h light / 16h dark periods (n=37-122). (**b**) Shoots of *A. thaliana d14-1*, with an empty vector (EV) or complemented with *AtD14, AtKAI2, LjD14, LjKAI2a* and *LjKAI2b*, driven by the *AtD14* promoter at 26 dpg. Scale bar = 10 cm. (**c**) Rosette branch number at 26 dpg of *A. thaliana* wild-type (Col-0), *d14-1* and *d14-1* lines carrying an empty vector (EV) or plasmids containing *AtD14, AtKAI2, LjD14, LjKAI2a* and *LjKAI2b*, driven by the *AtD14* promoter (n=24). Letters indicate different statistical groups (ANOVA, post-hoc Tukey test).

**Figure 3 | *Lotus japonicus* KAI2a, KAI2b and rice D14L confer divergent hypocotyl growth responses to $KAR_1$ and $KAR_2$ in Arabidopsis.**

(**a**) Structure of $KAR_1$, $KAR_2$, $GR24^{5DS}$ and $GR24^{ent\text{-}5DS}$. (**b-c**) Hypocotyl length of *A. thaliana kai2* mutants complemented with *KAI2* from *A. thaliana*, *L. japonicus* and rice, after treatment with solvent (Mock), 1µM of $KAR_1$ or $KAR_2$ at 6 dpg. (**b**) L*er* wild-type, *kai2-2* and *kai2-2* lines complemented with *AtKAI2, LjKAI2a* and *LjKAI2b*, driven by the *AtKAI2* promoter (n= 33-128). (**c**) L*er* and Col-0 wild-type, *htl-2* (Ler), K02821-line transgenic for *p35S:OsD14L* (Col-0), and two homozygous $F_3$ lines from the *htl-2* x K02821 cross [11] (n= 80-138). (**d**) Hypocotyl length of *A. thaliana* Col-0 wild-type, *d14-1 kai2-2* double mutants,

and *d14-1 kai2-2* lines complemented with *LjKAI2a* and *LjKAI2b*, driven by the *AtKAI2* promoter after treatment with solvent (Mock), 1µM GR24$^{5DS}$ or GR24$^{ent\text{-}5DS}$ (n= 59-134). (**b-d**) Seedlings were grown in 16h light / 8h dark periods. Letters indicate different statistical groups (ANOVA, post-hoc Tukey test).

**Figure 4 | Binding of GR24$^{ent\text{-}5DS}$ to LjKAI2a is determined by three amino acids.**

(**a**) The ligand-binding cavity regions of LjKAI2a and LjKAI2b proteins after structural homology modelling on the KAI2 crystal structure of *A. thaliana* [5]. Conserved residues in the cavity that differ between the KAI2a and KAI2b clades, and that are also different between LjKAI2b and AtKAI2, are shown in green. The phenylalanine residue in LjKAI2a, which is changed to tryptophan in LjKAI2b is shown in violet. The catalytic triad is coloured in red. (**b**) DSF curves of purified SUMO fusion proteins of wild-type LjKAI2a and LjKAI2b, and versions with swapped amino acids LjKAI2a$^{M160,L190}$, LjKAI2b$^{L161,S191}$, LjKAI2a$^{W157,M160,L190}$, LjKAI2b$^{F158,L161,S191}$, at the indicated concentrations of of GR24$^{ent\text{-}5DS}$. The first derivative of the change of fluorescence was plotted against the temperature. Each curve is the arithmetic mean of three sets of reactions, each comprising four technical replicates. Peaks indicate the protein melting temperature. The shift of the peak in LjKAI2a indicates ligand-induced thermal destabilisation consistent with a protein-ligand interaction. Insets plot the minimum value of (-dF/dT) at the melting point of the protein as determined in the absence of ligand (means ± SE, n = 3). Asterisks indicate significant differences to the solvent control (ANOVA, post-hoc Dunnett test, N.S.>0.05, *≤0.05, **≤0.01, ***≤0.001, ****≤0.0001).

**Figure 5 | Amino acid swaps reverse GR24$^{ent\text{-}5DS}$ LjKAI2b and LjKAI2b sensitivity in Arabidopsis hypocotyls.**

Hypocotyl length of *A. thaliana* Col-0 wild-type, *d14-1 kai2-2* double mutants, and *d14-1 kai2-2* lines complemented with *LjKAI2a* and *LjKAI2b* variants driven by the *AtKAI2* promoter and after treatment with solvent (Mock), 1 µM GR24$^{5DS}$ or GR24$^{ent\text{-}5DS}$. (**a**) *LjKAI2a*$^{M160,L190}$ and *LjKAI2a*$^{W157,M160,L190}$ (n = 46-84). (**b**) *LjKAI2b*$^{L161,S191}$ and *LjKAI2b*$^{F158,L161,S191}$ (n= 49-102). (**a-b**) Asterisks indicate significant differences versus mock treatment (Welch t.test, *≤0.05, **≤0.01, ***≤0.001, ****≤0.0001).

**Figure 6 | Role of *D14*, *KAI2a*, *KAI2b* and *MAX2* in shoot and hypocotyl development of *Lotus japonicus*.**

(**a**) Schematic representation of the *L. japonicus D14, KAI2a*, *KAI2b* and *MAX2* genes. Black boxes and lines show exons and introns, respectively. *LORE1* insertions are indicated by red triangles and EMS mutations by red stars. (**b**) Shoot phenotype of *L. japonicus* wild-type and karrikin and strigolactone perception mutants at 8 weeks post germination (wpg). Scale bars: 7 cm. (**c**) Number of branches of *L. japonicus* wild-type, karrikin and strigolactone perception mutants at 7 wpg (n = 12-21). (**d**) Hypocotyl length of the indicated genotypes of *L. japonicus* at 1 wpg (n = 79-97). (**c-d**) Letters indicate different statistical groups (ANOVA, post-hoc Tukey test).

**Figure 7 | *Lotus japonicus* hypocotyls respond to KAR$_1$ and KAR$_2$ in a *LjKAI2a*-dependent manner.**

(**a**) Hypocotyl length of *L. japonicus* seedling at 1 wpg after treatment with solvent (M) or three different concentrations of KAR$_1$, KAR$_2$ or *rac*-GR24 (GR24) (n= 95-105). Letters

indicate different statistical groups (ANOVA, post-hoc Tukey test). (**b**) Hypocotyl length of the indicated genotypes at 1 wpg after treatment with solvent (Mock), 1 µM $KAR_1$ or 1 µM $KAR_2$ (n = 73-107). (**c**) qRT-PCR-based expression of *DLK2* in hypocotyls at 1 wpg after 2 hours treatment with solvent (Mock), 1 µM $KAR_1$, 1 µM $KAR_2$, or 1 µM *rac*-GR24 (GR24) (n = 3). (**b-c**) Asterisks indicate significant differences of the compounds versus mock treatment (ANOVA, post-hoc Dunnett test, N.S.>0.05, *≤0.05, **≤0.01, ***≤0.001).

**Figure 8 | *Lotus japonicus* root system architecture is affected specifically by $KAR_1$ but not by $KAR_2$ treatment.**

(**a**) Primary root length (PRL), post-embryonic root (PER) number and PER density of wild-type plants 2 wpg after treatment with solvent (M) or three different concentrations of $KAR_1$, $KAR_2$ or *rac*-GR24 (GR24) (n = 32-57). (**b-c**) qRT-PCR-based expression of *DLK2* in roots at 2 wpg after 2 hours treatment with solvent (Mock), (**b**) 1 µM $KAR_1$ and 1 µM $KAR_2$, (**c**) 1 µM *rac*-GR24 (n = 4). (**a-b**) Letters indicate different statistical groups (ANOVA, post-hoc Tukey test). (**c**) Asterisk indicate significant differences versus mock treatment (Welch t.test, *≤0.05, **≤0.01, ***≤0.001).

**Figure 9 | *KAI2a* or *KAI2b* are redundantly required for $KAR_1$ response of roots.**

(**a**) Post-embryonic-root (PER) density of *L. japonicus* plants, 2 wpg after treatment with solvent (M) or 3µM $KAR_1$ (n=34-72). (**b**) qRT-PCR-based expression of *DLK2* in roots of *L. japonicus* plants at 2 wpg after 2 hours treatment with solvent (Mock) or 3 µM KAR1. (**a-b**) Asterisks indicate significant differences versus mock treatment (Welch t.test, *≤0.05, **≤0.01, ***≤0.001).

**Figure 10 | *L. japonicus* KAI2a and KAI2b diverge in ligand-binding specificity and organ-specific function.**

(**a**) KAI2a is required to mediate inhibition of hypocotyl growth in response to $KAR_1$ and $KAR_2$. In roots KAI2a and KAI2b redundantly promote lateral root density but only in response to $KAR_1$ treatment. (**b**) In the Arabidopsis *kai2-2* background LjKAI2a mediates hypocotyl growth inhibition to $KAR_1$, $KAR_2$ and GR24$^{ent\text{-}5DS}$. In the same background, LjKAI2b mediates a strong response to $KAR_1$, only a weak response to $KAR_2$ and no response to GR24$^{ent\text{-}5DS}$. However, swapping the three amino acids in the binding pocket that differ between LjKAI2a and LjKAI2b reconstitutes GR24$^{ent\text{-}5DS}$ activity through LjKAI2b, indicating that these three amino acids are decisive for GR24$^{ent\text{-}5DS}$ binding and/or receptor activation.

## Supplementary figure legends

**Supplementary Figure 1 | MAX2-like underwent pseudogenization.**

(**a**) Schematic representation of the synthenic regions containing the *MAX2* and *MAX2-like* loci in *L. japonicus*. Coloured arrows and black lines show exons and introns respectively. (**b**) Protein alignment of LjMAX2, LjMAX2-like and an artificial LjMAX2-like with a deletion of the thymine at the position 453 in the coding sequence (LjMAX2-like ΔT453). Position of the nucleotide deletion is indicated in the translated sequence by a red triangle. Amino-acid conservation between MAX2 and MAX2-like is indicated by a dark background.

**Supplementary Figure 2 | Organ-specific accumulation of *D14*, *KAI2a*, *KAI2b* and *MAX2* transcripts.**

(**a-c**) Transcript accumulation in wild-type of *D14*, *KAI2a*, *KAI2b* and *MAX2*, in (**a**) leaf, stem, flower and root of plants grown in pots, and in (**b**) hypocotyl and roots of 1 wpg plants grown on Petri dishes in 8h light / 16h dark cycles, and in (**c**) roots of 2 wpg plants grown on Petri dishes in 16h light / 8h dark cycles (n = 3).

**Supplementary Figure 3 | Subcellular localisation of LjD14, LjKAI2a, LjKAI2b and LjMAX2 in *Nicotiana benthamiana* leaves.**

(**a**) Subcellular localization of LjD14, LjKAI2a, LjKAI2b and LjMAX2 in *N. benthamiana* leaf epidermal cells. LjD14, LjKAI2a and LjKAI2b are N-terminally fused with mOrange. LjMAX2 is N-terminally fused with T-Sapphire. Scale bars: 25 μm. (**b**) Western blot of protein extracts from *N. benthamiana*, showing that the mOrange tag fused with LjD14, LjKAI2a and LjKAI2b was not cleaved at detectable amounts.

**Supplementary Figure 4 | SDS-PAGE of purified SUMO fusion proteins.**

200 pmol (approx. 8 μg) of purified proteins were separated by 12% SDS-PAGE containing 2,2,2 trichlorethanol as a vizualization agent. Below each lane is the calculated protein size in kiloDaltons. S, protein size standards (Precision Plus Dual Color Standards, Bio-Rad #1610394) with corresponding sized in kDa shown on the left. Optimal exposures of recombinant proteins and size standards were taken separately under UV transillumination and red epi-illumination, respectively. The two images were merged in post-processing, and the junction between them is indicated by a vertical line.

**Supplementary Figure 5 | Amino acid differences between the legume KAI2a and KAI2b clades.**

Protein sequence alignment of KAI2a and KAI2b homologs from the legumes *Lotus japonicus, Pisum sativum, Medicago truncatula* and *Glycine max*, in comparison with Arabidopsis KAI2 and rice D14L. Residues conserved within the KAI2a and KAI2b clades but different between these clades are coloured in green and blue. Residues of the catalytic triad are coloured in red. A non-conserved tryptophan in LjKAI2b located in the protein cavity is coloured in violet. Yellow and orange triangles indicate amino acid residues located in the ligand-binding cavity of the proteins. Orange triangles indicate the three amino acids responsible for differences in GR24$^{ent\text{-}5DS}$-binding between LjKAI2a and LjKAI2b.

**Supplementary Figure 6 | Transcript accumulation in the *L. japonicus* KAR and SL receptor mutants.**

(**a**) qRT-PCR based transcript accumulation of *LjKAI2a* and *LjKAI2b*, in roots of wild type and *kai2a-1*, *kai2b-1*, *kai2b-3*, *kai2a-1 kai2b-1* and *max2-4* as well as *LjMAX2* and *LjD14* in *max2-4* and *d14-1*, respectively (n=4). (**b**) *LjKAI2*b transcript accumulation in wild-type, *kai2b-1* (stop codon) and *kai2b-3* (LORE1 insertion) mutants by semi-quantitative RT-PCR using primer pairs located 5' and 3' of the mutations, as well as flanking (ML) the mutations. Transcript accumulation of the housekeeping gene Ubiquitin is also shown.

**Supplementary Figure 7 | Characterisation of the *kai2a-1* allele.**

(**a**) Schematic representation of mis-splicing caused by the LORE1 insertion in the *kai2a-1* mutant. (**b**) cDNA alignment showing the absence of nucleotides 369 to 383 in the *kai2a-1* transcript, causing a deletion of amino acids 124 to 128 (orange). (**c**) Protein model of LjKAI2a based on the AtKAI2-KAR$_1$ complex 4JYM [5] showing KAR$_1$ in green, residues of

the catalytic triad in red and the amino acids missing in a hypothetical LjKAI2a-1 protein in orange. (**d**) Hypocotyl elongation at 6 dpg in Arabidopsis *kai2-2* mutants transgenically complemented with genomic and the cDNA of wild-type *LjKAI2a* and *Ljkai2a-1* driven by the *AtKAI2* promoter (n = 75-106). Plants were grown in 8h light / 16h dark cycles. Letters indicate different statistical groups (ANOVA, post-hoc Tukey test).

**Supplementary Figure 8 | Suppression of *L. japonicus* hypocotyl growth by KAR treatment depends on *MAX2*.**

(**a**) Hypocotyl length of wild-type and *max2-4* seedlings one-week post germination after treatment with solvent (Mock), 1 µM $KAR_1$, 1 µM $KAR_2$ (n = 66-96). Asterisks indicate significant differences of the compounds versus mock treatment (ANOVA, post-hoc Dunnett test, N.S.>0.05, *≤0.05, **≤0.01, ***≤0.001). (**b**) Comparison of *DLK2* transcript accumulation in hypocotyls of mock treated wild-type, *kai2a-1, kai2b-3, kai2a-1 kai2b-1* and *max2-4* displayed in Fig 7C (n=3). Letters indicate different statistical groups (ANOVA, post-hoc Tukey test).

**Supplementary Figure 9 | Refreshing *rac*-GR24 in the medium does not influence root architecture.**

PER density of wild-type plants at 2 wpg and treated with solvent (Mock) 1 µM $KAR_1$, 1 µM $KAR_2$, or 1 µM *rac*-GR24 (n = 43-51). Plants were transferred onto fresh hormone-containing medium after 5 days. Asterisks indicate significant differences (ANOVA, Dunnett test, N.S.>0.05, *≤0.05).

**Supplementary Figure 10 | Small overlap between transcriptional responses of *Lotus japonicus* roots to $KAR_1$ and *rac*-GR24.**

Number of differentially expressed genes (DEGs, adjusted p-value < 0.01) as assessed by microarray analysis. Left panel: DEGs responding to 1 µM $KAR_1$ after 1h, 2h and 6h incubation. Middle panel: DE genes responding to 1 µM *rac*-GR24 1h, 2, 6h incubation. Right panel: comparison of DE genes responding to 2 h treatment with $KAR_1$ and *rac*-GR24.

**Supplementary Figure 11 | KAR perception mutants are less responsive to $KAR_1$ treatment.**

(**a-c**) Post-embryonic-root (PER) density of *L. japonicus* plants, 2 wpg after treatment with solvent (Mock) or 1 µM $KAR_1$, of wild-type, (**a**) *kai2a-1*, *kai2b-1* and *kai2a-1 kai2b-1* (n= 32-50); (**b**) *max2-4* (n= 34-43); (**c**) *kai2a-1*, *kai2b-3* and *kai2a-1 kai2b-1* (n= 37-72). (**a-c**) Asterisks indicate significant differences versus mock treatment (Welch t.test, *≤0.05, **≤0.01, ***≤0.001).

**Supplementary Figure 12 | $KAR_1$ response in roots requires *LjKAI2a* or *LjKAI2b* and *LjMAX2*.**

Primary-root length (PRL) and post-embryonic-root (PER) number of *L. japonicus* plants, 2 wpg after treatment with solvent (Mock) or 3 µM $KAR_1$ (n=34-72) displayed in Fig 9A. Asterisks indicate significant differences versus mock treatment (Welch t.test, *≤0.05, **≤0.01, ***≤0.001).

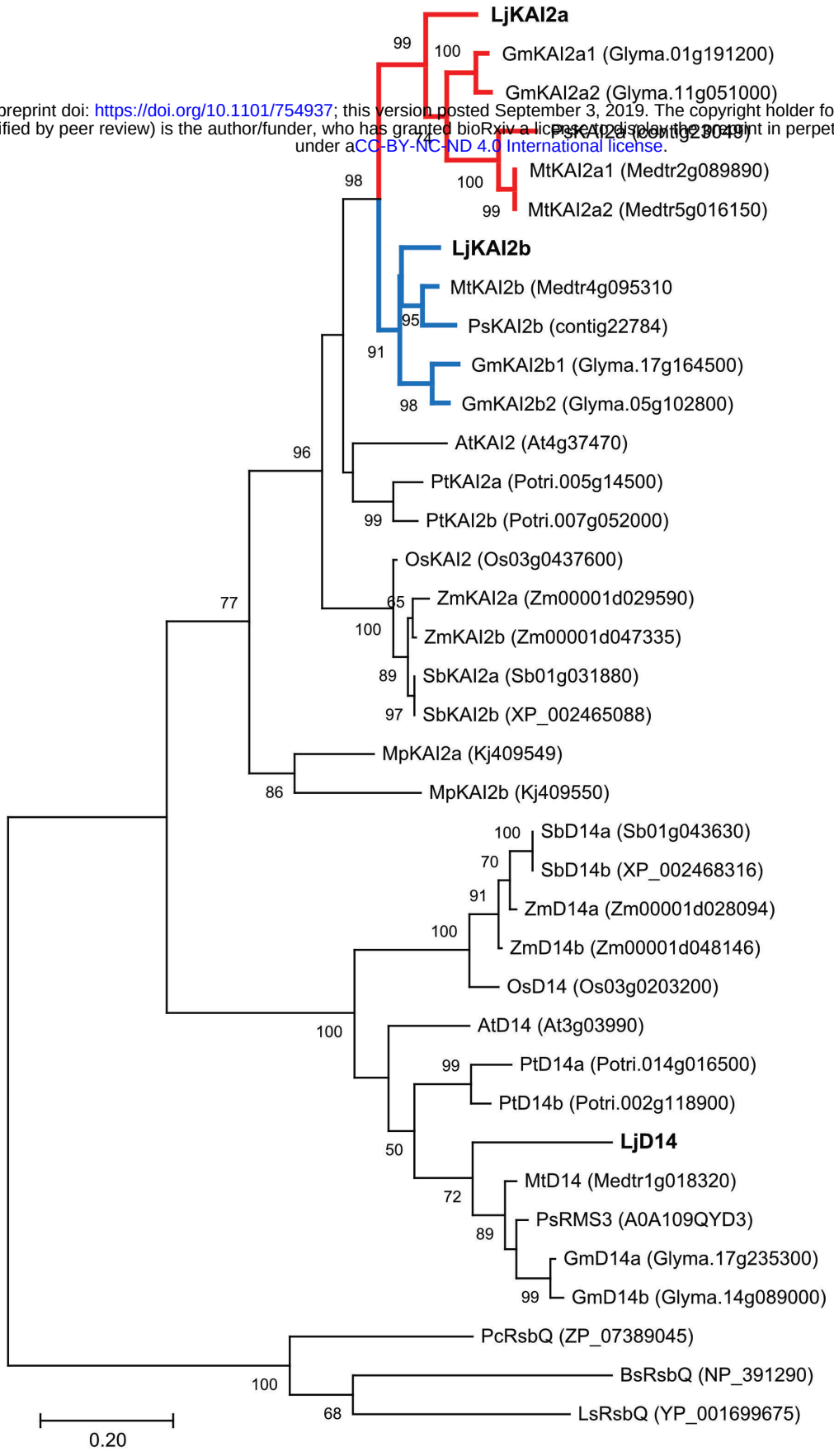


**Figure 1 | The KAI2 gene underwent duplication prior to diversification of the legumes.**

Phylogenetic tree of KAI2 and D14 rooted with bacterial RbsQ from indicated species (*Lj, Lotus japonicus; Gm, Glycine max; Ps, Pisum sativum; Mt, Medicago truncatula; At, Arabidopsis thaliana; Pt, Populus trichocarpa; Os, Oryza sativa; Zm, Zea mays; Sb, Sorghum bicolor; Mp, Marchantia polymorpha*). Protein sequences were aligned using MAFFT. MEGA7 was used to generate a tree inferred by Maximum Likelihood method. The tree with the highest log likelihood (-6038.38) is shown. The percentage of trees in which the associated taxa clustered together is shown next to the branches. Values below 50 were ignored. *KAI2* duplication in the legumes is highlighted by red and blue branches.

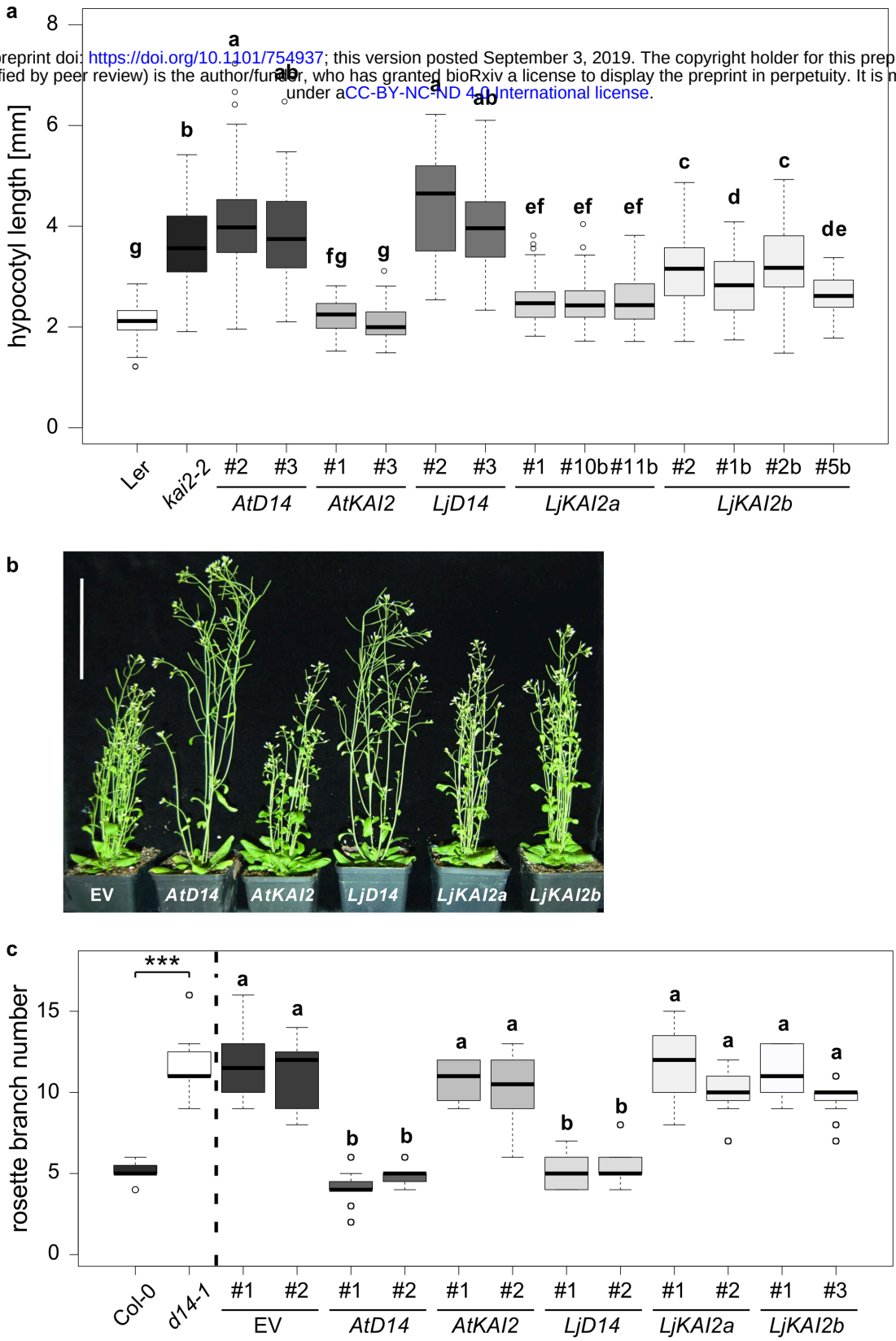


**Figure 2 | *Lotus japonicus D14*, *KAI2a* and *KAI2b* can replace *D14* and *KAI2* in Arabidopsis, respectively.**

(**a**) Hypocotyl length of *A. thaliana* wild-type (L*er*), *kai2-2* and *kai2-2* lines complemented by *AtD14, AtKAI2, LjD14, LjKAI2a* and *LjKAI2b*, driven by the *AtKAI2* promoter at 6 days post germination (dpg). Seedlings were grown in 8h light / 16h dark periods (n=37-122). (**b**) Shoots of *A. thaliana d14-1*, with an empty vector (EV) or complemented with *AtD14, AtKAI2, LjD14, LjKAI2a* and *LjKAI2b*, driven by the *AtD14* promoter at 26 dpg. Scale bar = 10 cm. (**c**) Rosette branch number at 26 dpg of *A. thaliana* wild-type (Col-0), *d14-1* and *d14-1* lines carrying an empty vector (EV) or plasmids containing *AtD14, AtKAI2, LjD14, LjKAI2a* and *LjKAI2b*, driven by the *AtD14* promoter (n=24). Letters indicate different statistical groups (ANOVA, post-hoc Tukey test).

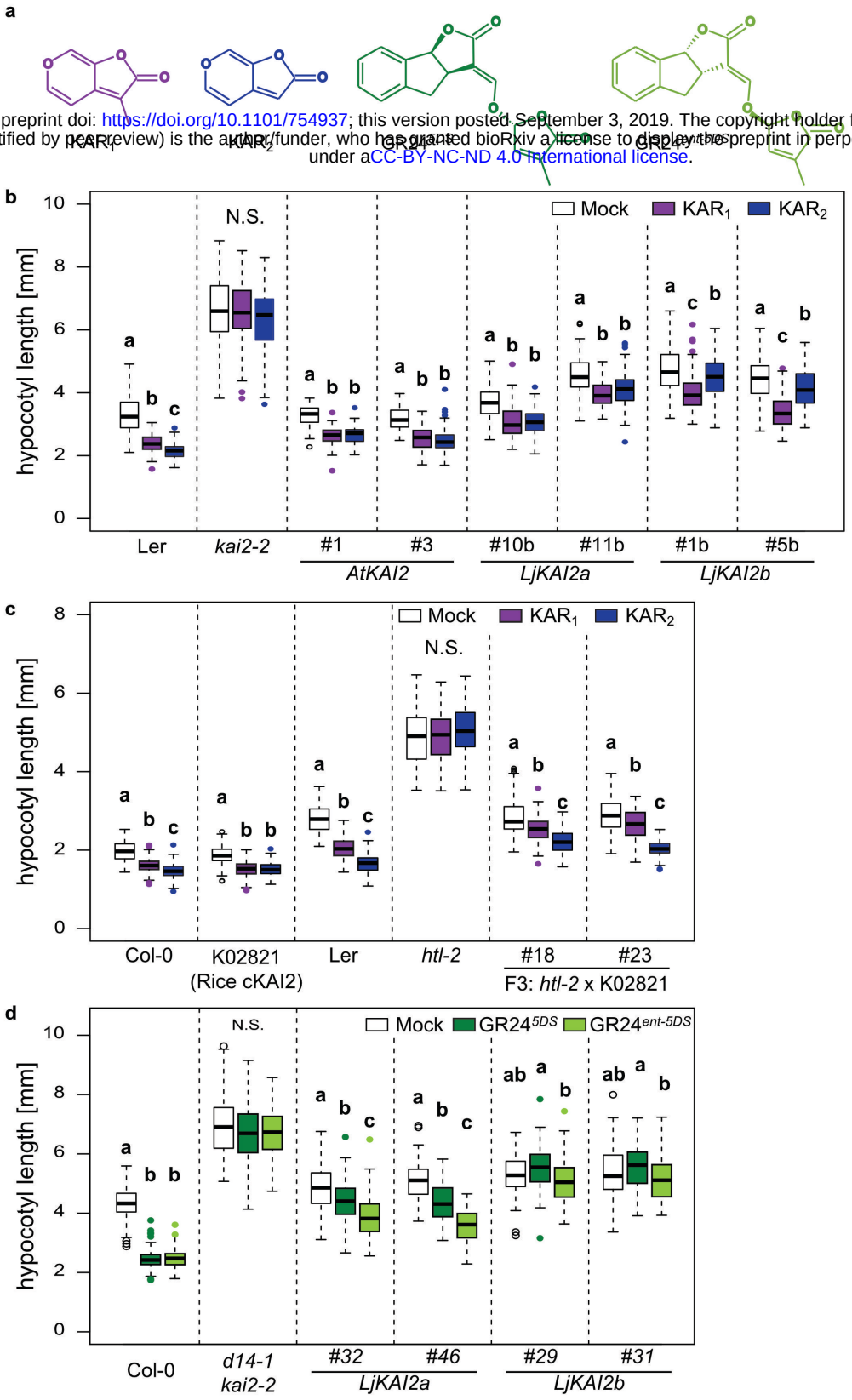


**Figure 3 | *Lotus japonicus* KAI2a, KAI2b and rice D14L confer divergent hypocotyl growth responses to $KAR_1$ and $KAR_2$ in Arabidopsis.**

(**a**) Structure of $KAR_1$, $KAR_2$, $GR24^{5DS}$ and $GR24^{ent\text{-}5DS}$. (**b-c**) Hypocotyl length of *A. thaliana kai2* mutants complemented with *KAI2* from *A. thaliana*, *L. japonicus* and rice, after treatment with solvent (Mock), 1µM of $KAR_1$ or $KAR_2$ at 6 dpg. (**b**) L*er* wild-type, *kai2-2* and *kai2-2* lines complemented with *AtKAI2, LjKAI2a* and *LjKAI2b*, driven by the *AtKAI2* promoter (n= 33-128). (**c**) L*er* and Col-0 wild-type, *htl-2* (Ler), K02821-line transgenic for *p35S:OsD14L* (Col-0), and two homozygous $F_3$ lines from the *htl-2* x K02821 cross [11] (n= 80-138). (**d**) Hypocotyl length of *A. thaliana* Col-0 wild-type, *d14-1 kai2-2* double mutants, and *d14-1 kai2-2* lines complemented with *LjKAI2a* and *LjKAI2b*, driven by the *AtKAI2* promoter after treatment with solvent (Mock), 1µM $GR24^{5DS}$ or $GR24^{ent\text{-}5DS}$ (n= 59-134). (**b-d**) Seedlings were grown in 16h light / 8h dark periods. Letters indicate different statistical groups (ANOVA, post-hoc Tukey test).

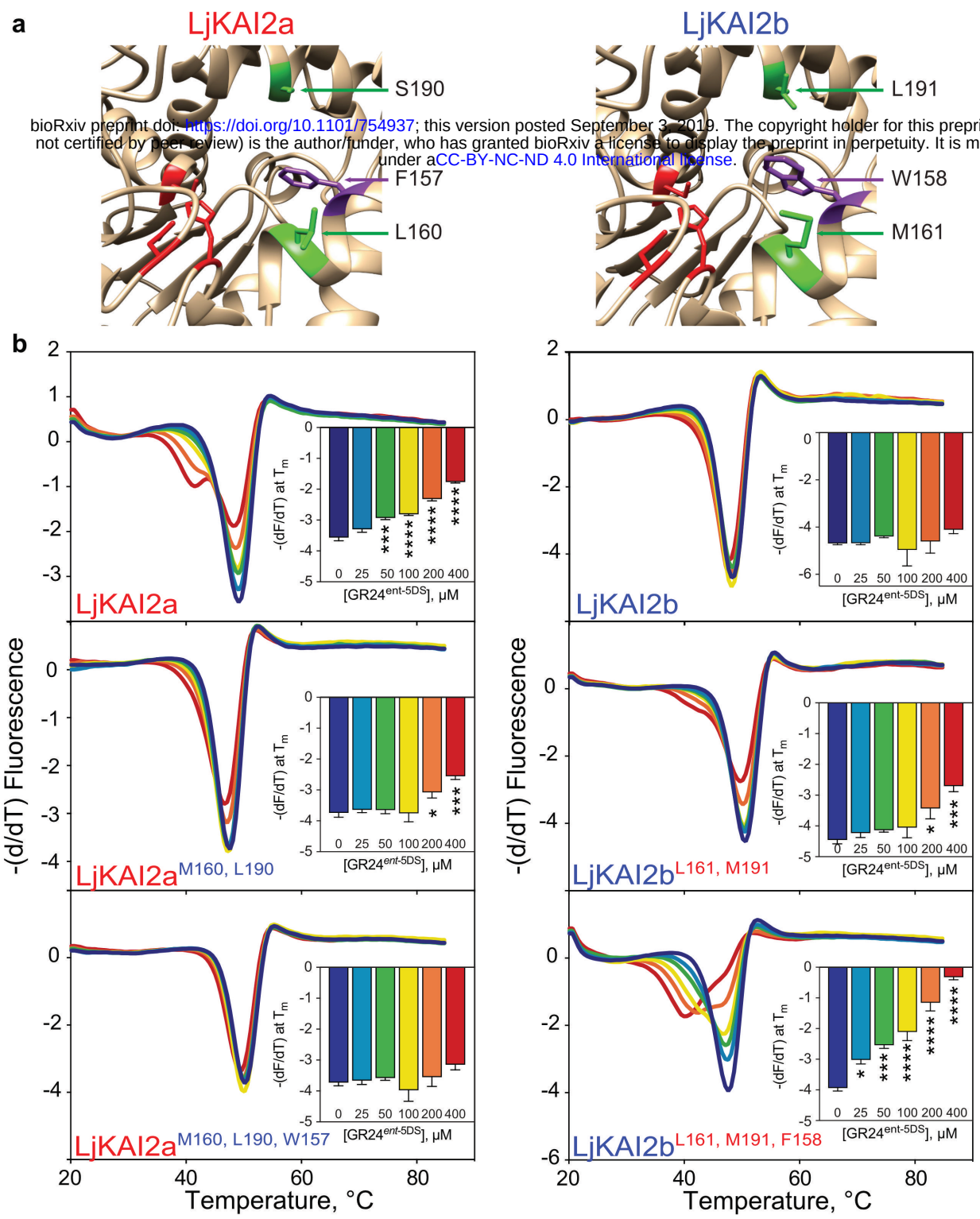


**Figure 4 | Binding of GR24$^{ent\text{-}5DS}$ to LjKAI2a is determined by three amino acids.**

(**a**) The ligand-binding cavity regions of LjKAI2a and LjKAI2b proteins after structural homology modelling on the KAI2 crystal structure of *A. thaliana* [5]. Conserved residues in the cavity that differ between the KAI2a and KAI2b clades, and that are also different between LjKAI2b and AtKAI2, are shown in green. The phenylalanine residue in LjKAI2a, which is changed to tryptophan in LjKAI2b is shown in violet. The catalytic triad is coloured in red. (**b**) DSF curves of purified SUMO fusion proteins of wild-type LjKAI2a and LjKAI2b, and versions with swapped amino acids LjKAI2a$^{M160,L190}$, LjKAI2b$^{L161,S191}$, LjKAI2a$^{W157,M160,L190}$, LjKAI2b$^{F158,L161,S191}$, at the indicated concentrations of of GR24$^{ent\text{-}5DS}$. The first derivative of the change of fluorescence was plotted against the temperature. Each curve is the arithmetic mean of three sets of reactions, each comprising four technical replicates. Peaks indicate the protein melting temperature. The shift of the peak in LjKAI2a indicates ligand-induced thermal destabilisation consistent with a protein-ligand interaction. Insets plot the minimum value of (-dF/dT) at the melting point of the protein as determined in the absence of ligand (means ± SE, n = 3). Asterisks indicate significant differences to the solvent control (ANOVA, post-hoc Dunnett test, N.S.>0.05, *≤0.05, **≤0.01, ***≤0.001, ****≤0.0001).

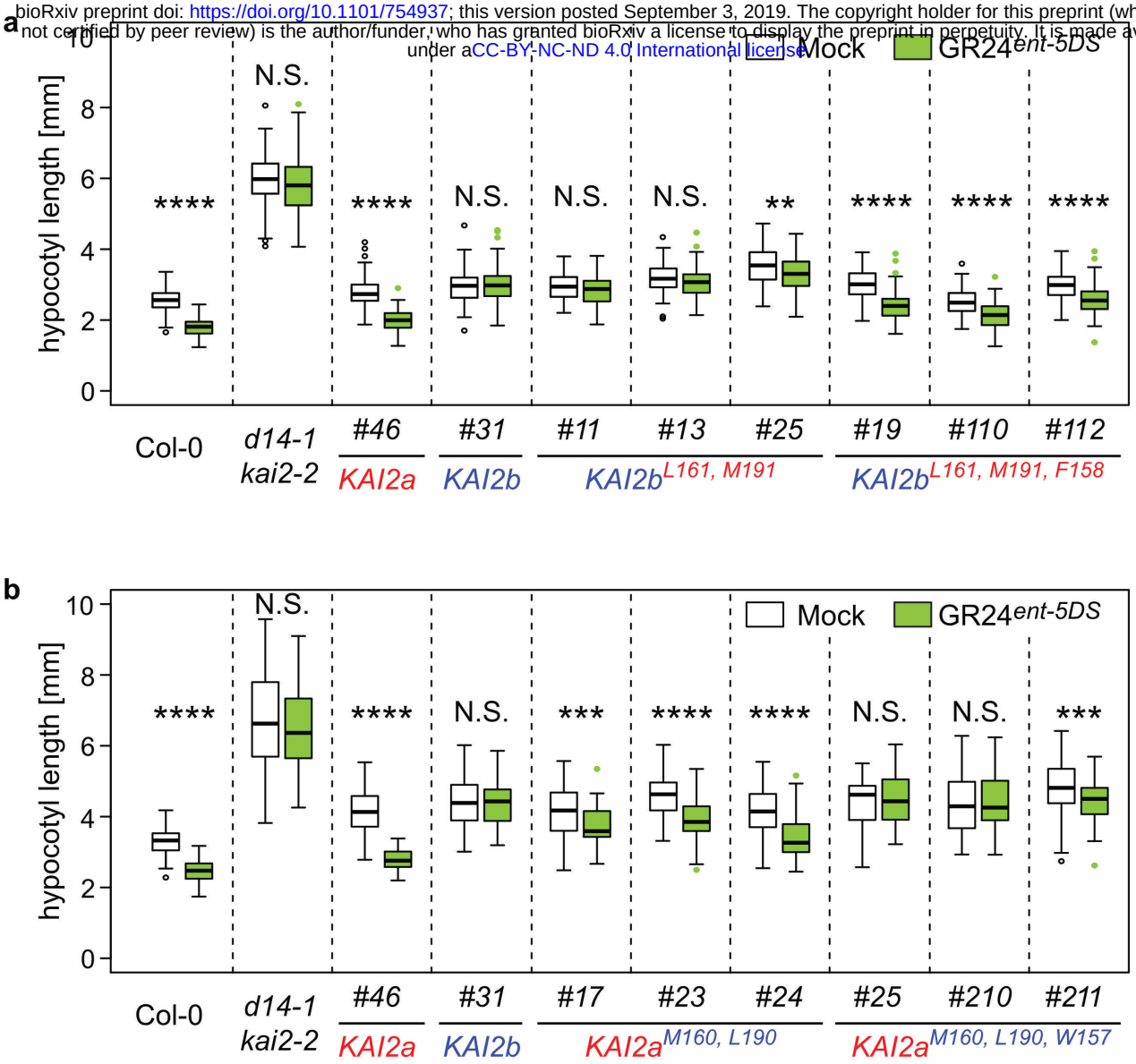


**Figure 5 | Amino acid swaps reverse GR24$^{ent\text{-}5DS}$ LjKAI2b and LjKAI2b sensitivity in Arabidopsis hypocotyls.**

Hypocotyl length of *A. thaliana* Col-0 wild-type, *d14-1 kai2-2* double mutants, and *d14-1 kai2-2* lines complemented with *LjKAI2a* and *LjKAI2b* variants driven by the *AtKAI2* promoter and after treatment with solvent (Mock), 1 µM GR24$^{5DS}$ or GR24$^{ent\text{-}5DS}$. (**a**) *LjKAI2a*$^{M160,L190}$ and *LjKAI2a*$^{W157,M160,L190}$ (n = 46-84). (**b**) *LjKAI2b*$^{L161,S191}$ and *LjKAI2b*$^{F158,L161,S191}$ (n= 49-102). (**a-b**) Asterisks indicate significant differences versus mock treatment (Welch t.test, *≤0.05, **≤0.01, ***≤0.001, ****≤0.0001).

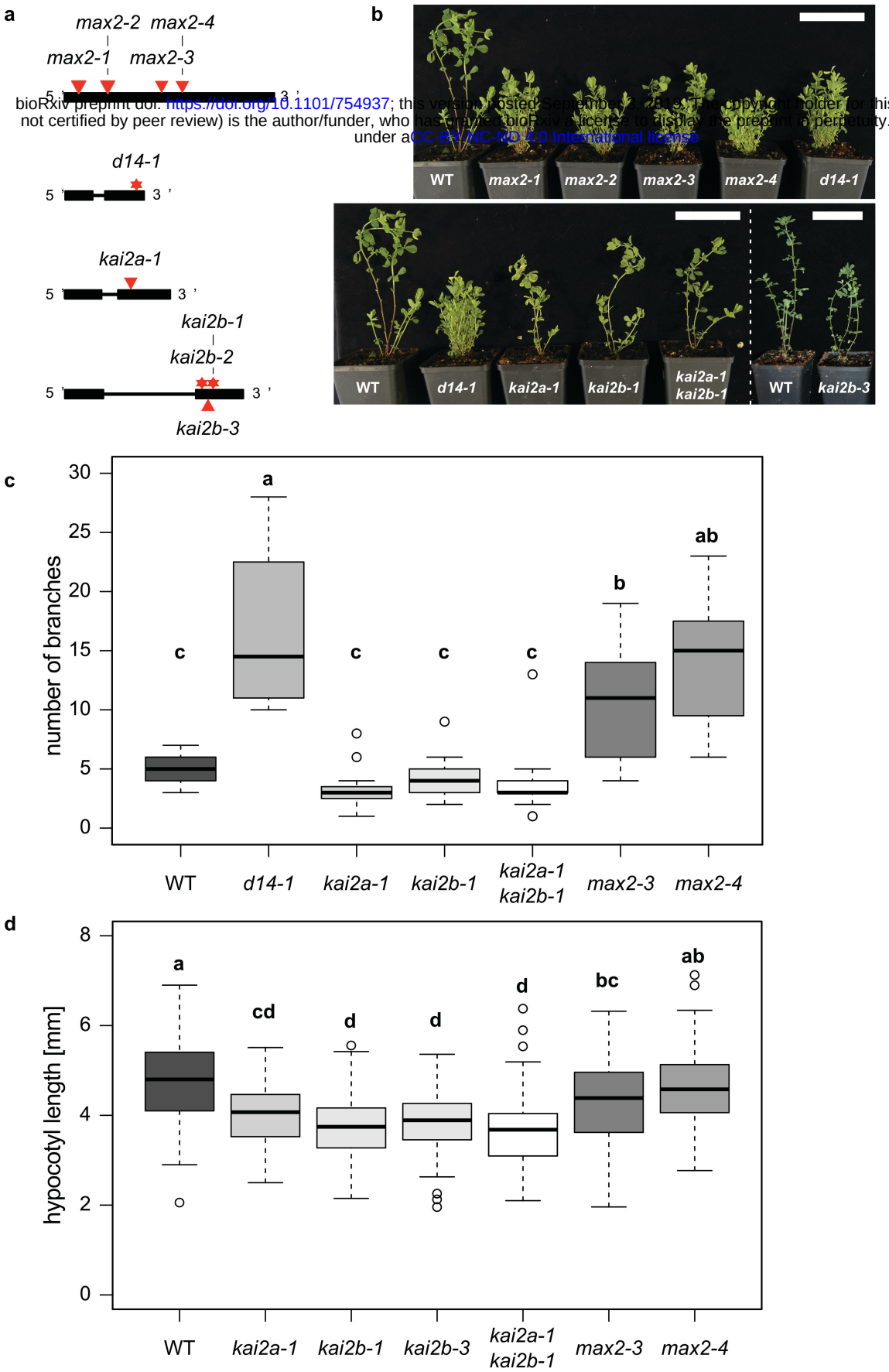


**Figure 6 | Role of *D14*, *KAI2a*, *KAI2b* and *MAX2* in shoot and hypocotyl development of *Lotus japonicus*.**

(**a**) Schematic representation of the *L. japonicus D14, KAI2a*, *KAI2b* and *MAX2* genes. Black boxes and lines show exons and introns, respectively. *LORE1* insertions are indicated by red triangles and EMS mutations by red stars. (**b**) Shoot phenotype of *L. japonicus* wild-type and karrikin and strigolactone perception mutants at 8 weeks post germination (wpg). Scale bars: 7 cm. (**c**) Number of branches of *L. japonicus* wild-type, karrikin and strigolactone perception mutants at 7 wpg (n = 12-21). (**d**) Hypocotyl length of the indicated genotypes of *L. japonicus* at 1 wpg (n = 79-97). (**c-d**) Letters indicate different statistical groups (ANOVA, post-hoc Tukey test).

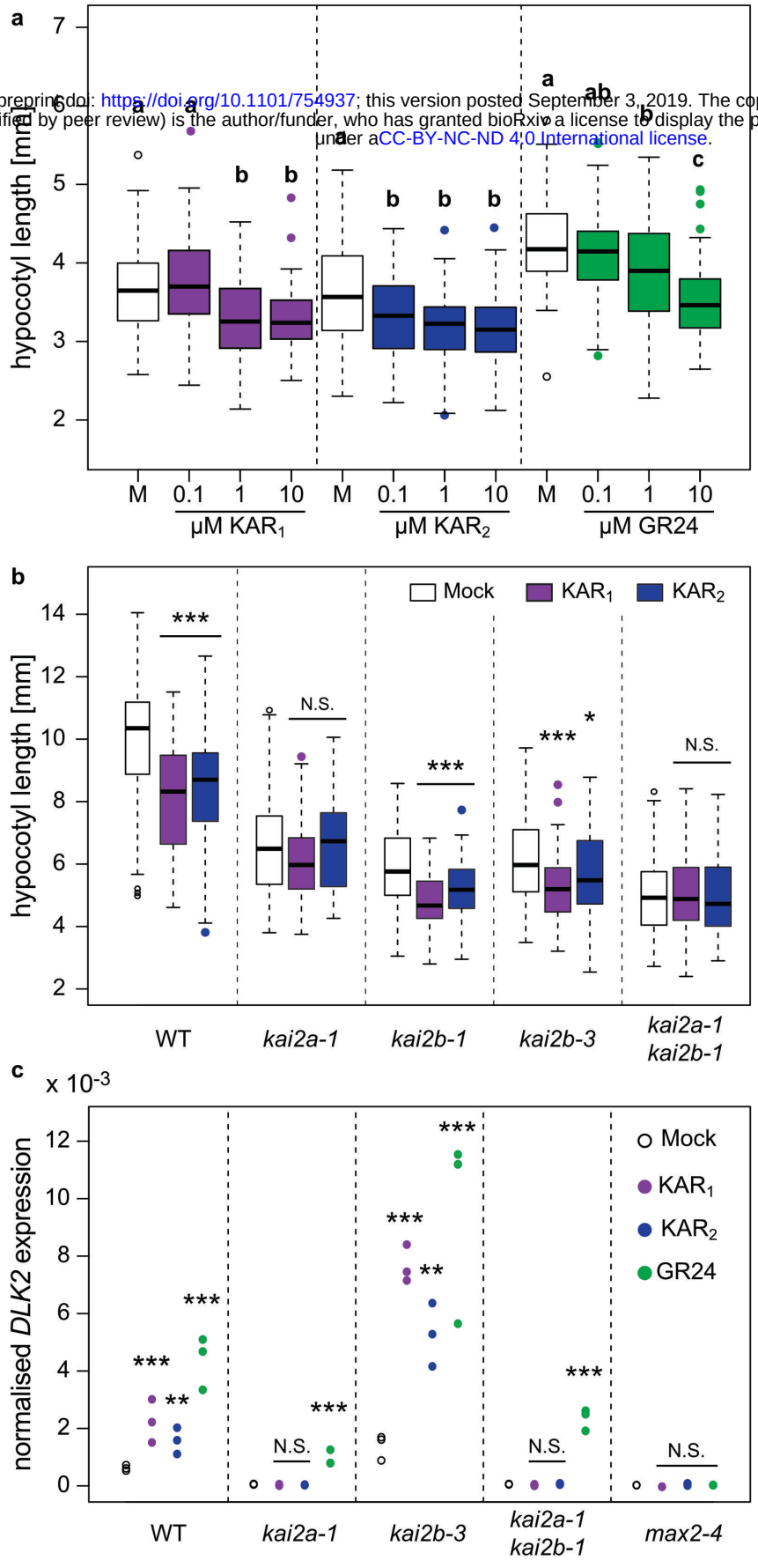


**Figure 7 | *Lotus japonicus* hypocotyls respond to $KAR_1$ and $KAR_2$ in a *LjKAI2a*- dependent manner.**

(**a**) Hypocotyl length of *L. japonicus* seedling at 1 wpg after treatment with solvent (M) or three different concentrations of $KAR_1$, $KAR_2$ or *rac*-GR24 (GR24) (n= 95-105). Letters indicate different statistical groups (ANOVA, post-hoc Tukey test). (**b**) Hypocotyl length of the indicated genotypes at 1 wpg after treatment with solvent (Mock), 1 µM $KAR_1$ or 1 µM $KAR_2$ (n = 73-107). (**c**) qRT-PCR-based expression of *DLK2* in hypocotyls at 1 wpg after 2 hours treatment with solvent (Mock), 1 µM $KAR_1$, 1 µM $KAR_2$, or 1 µM *rac*-GR24 (GR24) (n = 3). (**b-c**) Asterisks indicate significant differences of the compounds versus mock treatment (ANOVA, post-hoc Dunnett test, N.S.>0.05, *≤0.05, **≤0.01, ***≤0.001).

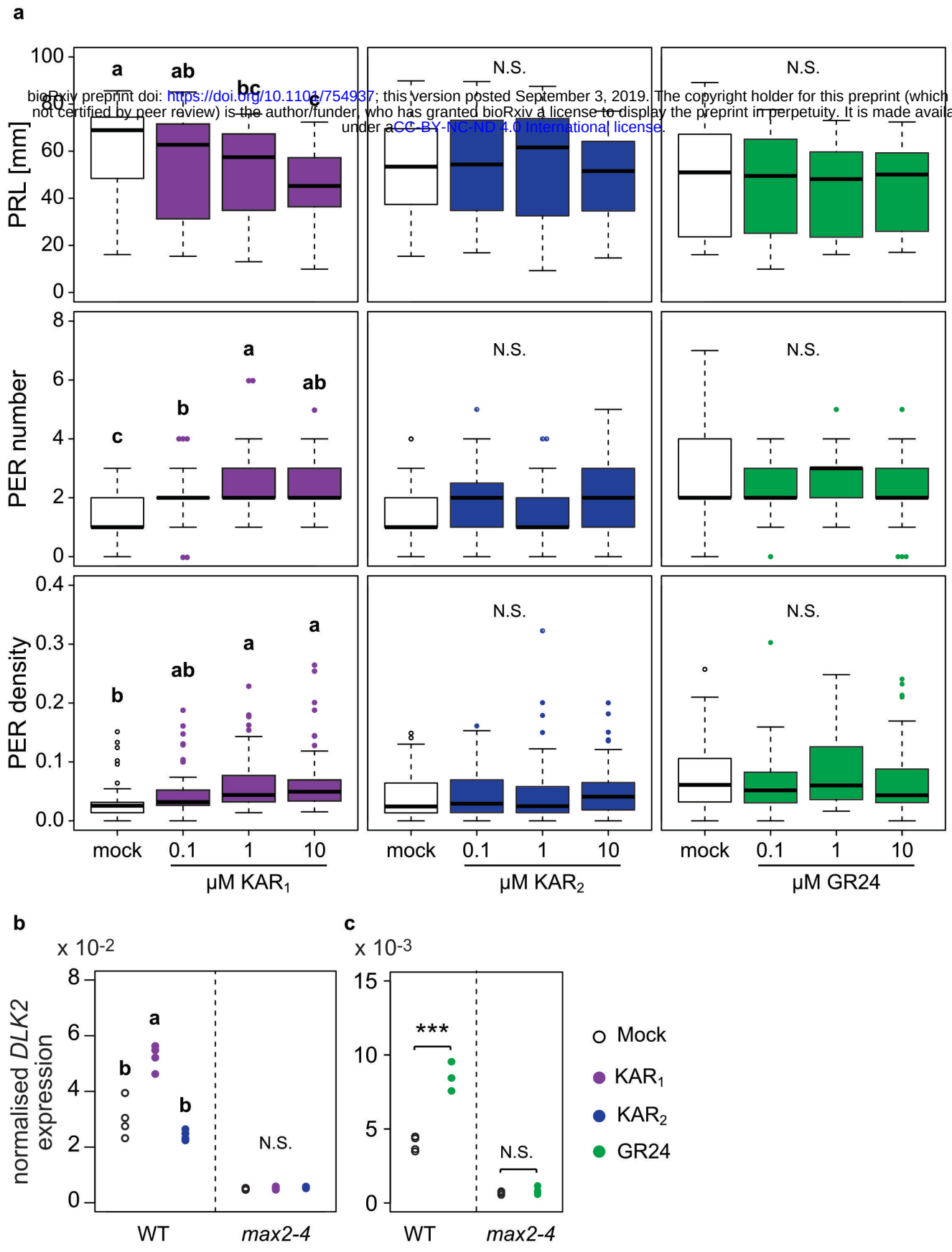


**Figure 8 | *Lotus japonicus* root system architecture is affected specifically by $KAR_1$ but not by $KAR_2$ treatment.**

(**a**) Primary root length (PRL), post-embryonic root (PER) number and PER density of wild-type plants 2 wpg after treatment with solvent (M) or three different concentrations of $KAR_1$, $KAR_2$ or *rac*-GR24 (GR24) (n = 32-57). (**b-c**) qRT-PCR-based expression of *DLK2* in roots at 2 wpg after 2 hours treatment with solvent (Mock), (**b**) 1 µM $KAR_1$ and 1 µM $KAR_2$, (**c**) 1 µM *rac*-GR24 (n = 4). (**a-b**) Letters indicate different statistical groups (ANOVA, post-hoc Tukey test). (**c**) Asterisk indicate significant differences versus mock treatment (Welch t.test, *≤0.05, **≤0.01, ***≤0.001).

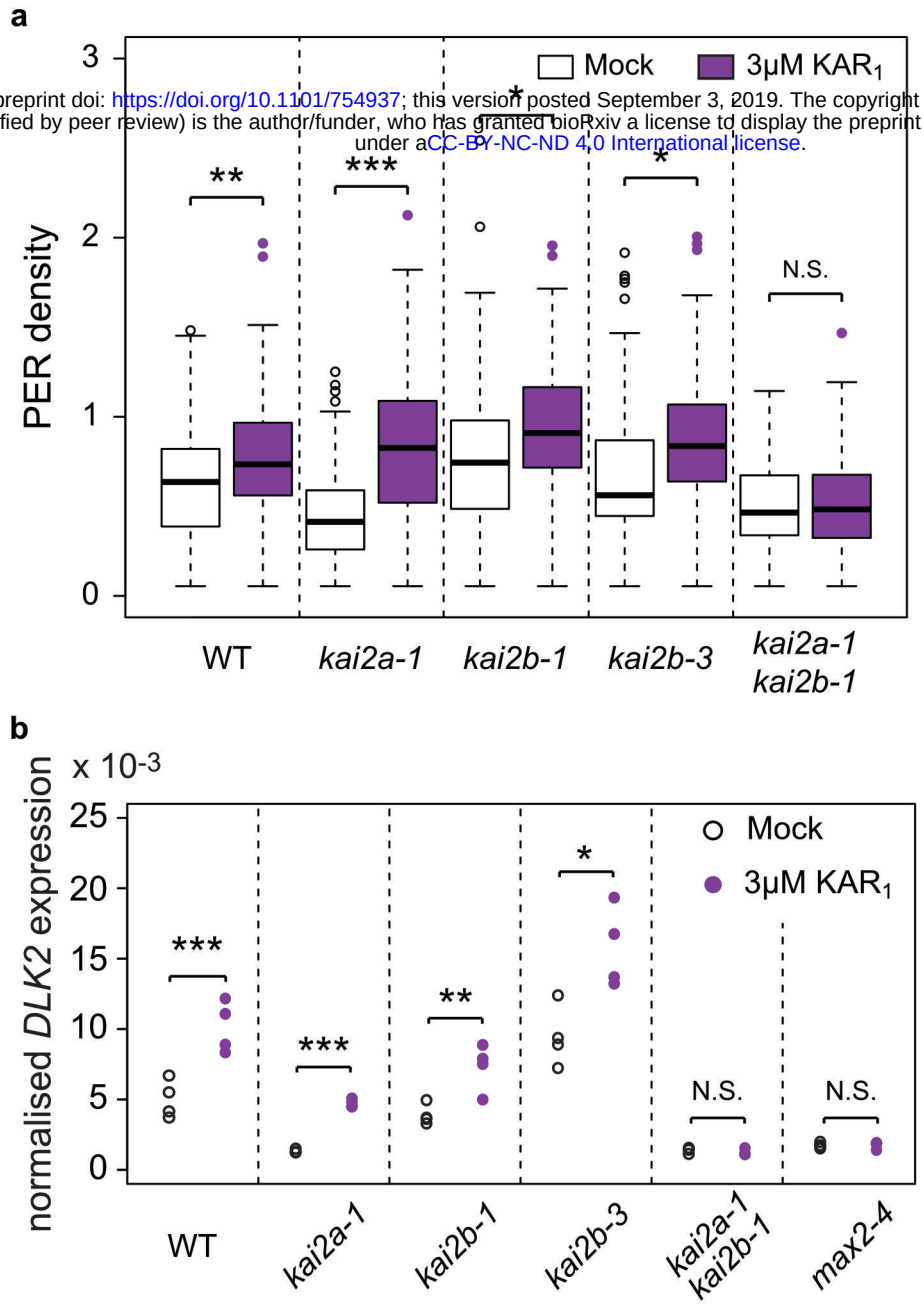


**Figure 9 | *KAI2a* or *KAI2b* are redundantly required for $KAR_1$ response of roots.**

(**a**) Post-embryonic-root (PER) density of *L. japonicus* plants, 2 wpg after treatment with solvent (M) or 3μM $KAR_1$ (n=34-72). (**b**) qRT-PCR-based expression of *DLK2* in roots of *L. japonicus* plants at 2 wpg after 2 hours treatment with solvent (Mock) or 3 μM KAR1. (**a-b**) Asterisks indicate significant differences versus mock treatment (Welch t.test, *≤0.05, **≤0.01, ***≤0.001).

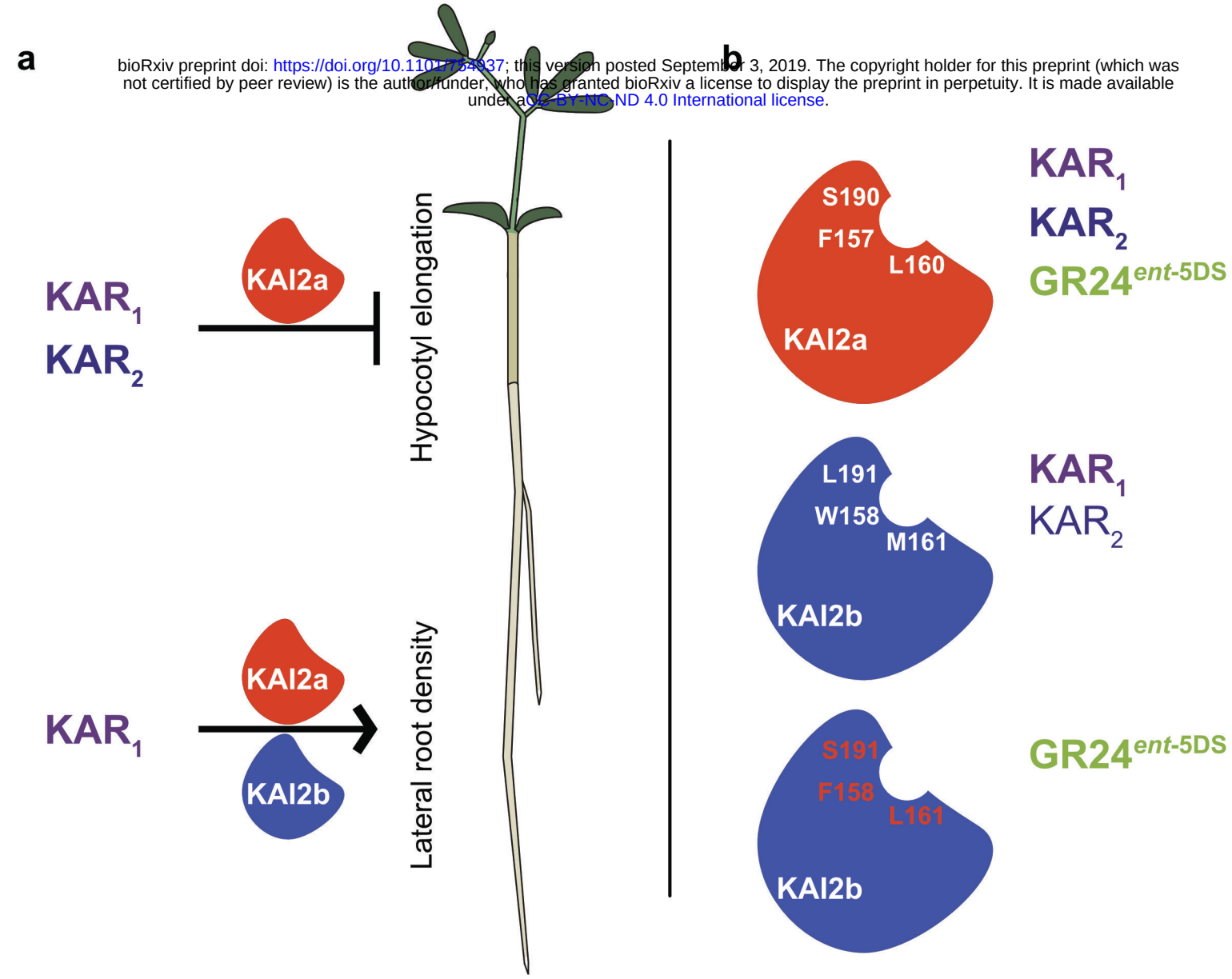


**Figure 10 | *L. japonicus* KAI2a and KAI2b diverge in ligand-binding specificity and organ-specific function.**

(**a**) KAI2a is required to mediate inhibition of hypocotyl growth in response to $KAR_1$ and $KAR_2$. In roots KAI2a and KAI2b redundantly promote lateral root density but only in response to $KAR_1$ treatment. (**b**) In the Arabidopsis *kai2-2* background LjKAI2a mediates hypocotyl growth inhibition to $KAR_1$, $KAR_2$ and $GR24^{ent\text{-}5DS}$. In the same background, LjKAI2b mediates a strong response to $KAR_1$, only a weak response to $KAR_2$ and no response to $GR24^{ent\text{-}5DS}$. However, swapping the three amino acids in the binding pocket that differ between LjKAI2a and LjKAI2b reconstitutes $GR24^{ent\text{-}5DS}$ activity through LjKAI2b, indicating that these three amino acids are decisive for $GR24^{ent\text{-}5DS}$ binding and/or receptor activation.